

**BRITISH GEOLOGICAL SURVEY**  
**TECHNICAL REPORT**  
**Mineralogy & Petrology Series**

**REPORT NO. WG/98/4R**

**THE MINERALOGY AND PETROGRAPHY**  
**OF THE LAMBETH GROUP**  
**FROM THE LONDON AND HAMPSHIRE BASINS**

**J M Pearce, S J Kemp and V L Hards**

**Date**

July 2, 1999

**Classification**

Restricted

**Geographical index**

Essex, Berkshire, Hampshire, Isle of Wight UK

**Subject index**

Clay minerals, X-ray diffraction analysis, scanning electron microscopy

**Bibliographic reference**

Pearce, J.M., Kemp S.J. and Hards, V.L. 1999. The mineralogy and petrography of the Lambeth Group from the London and Hampshire basins. *British Geological Survey Technical Report WG/98/4R*

This report has been generated from a scanned image of the document with any blank pages removed at the scanning stage.  
Please be aware that the pagination and scales of diagrams or maps in the resulting report may not appear as in the original

## CONTENTS

	Page
<b>1. INTRODUCTION</b>	<b>1</b>
<b>2. SAMPLES</b>	<b>3</b>
<b>3. LABORATORY METHODS</b>	<b>4</b>
3.1. X-ray diffraction (XRD) analysis	4
3.2. Scanning electron microscopy (SEM) analysis	5
3.3. Surface area determination	6
<b>4. RESULTS</b>	<b>6</b>
4.1. Summary of mineralogy	6
4.2. The London Basin	7
4.2.1. Thanet Sands	7
4.2.2. The Upnor Formation	7
4.2.3. The Reading Formation	11
4.2.4. The Woolwich Formation	14
4.3. Summary of mineralogy and petrography in the London Basin	15
4.3.1. Upnor Formation	15
4.3.2. Reading Formation	16
4.3.3. Woolwich Formation	16
4.4. The Hampshire Basin	16
4.5. Summary of mineralogy and petrography in the Hampshire Basin	19
4.5.1. Upnor Formation	19
4.5.2. Reading Formation	19
<b>5. DISCUSSION</b>	<b>19</b>
5.1. The London Basin	19
5.2. The Hampshire Basin	20
5.3. Origin of clay minerals	21
5.4. Mineralogical and petrographical controls on engineering properties	22
<b>6. CONCLUSIONS</b>	<b>23</b>
<b>7. REFERENCES</b>	<b>24</b>

## TABLES

	Page
<b>Table 1. Sample localities and descriptions (London Basin)</b>	<b>26</b>
<b>Table 2. Sample localities and descriptions (Jubilee Line Extension BH 404T)</b>	<b>27</b>

<b>Table 3. Sample localities and descriptions (Hampshire Basin)</b>	<b>27</b>
<b>Table 4. Summary of whole-rock XRD and surface area analyses (London Basin)</b>	<b>28</b>
<b>Table 5. Summary of whole-rock XRD and surface area analyses (Hampshire Basin)</b>	<b>30</b>
<b>Table 6. Summary of surface area analyses (Jubilee Line Extension BH 404T)</b>	<b>31</b>
<b>Table 7. Summary of &lt;2 µm XRD analyses (London Basin)</b>	<b>32</b>
<b>Table 8. Summary of &lt;2 µm XRD analyses (Hampshire Basin)</b>	<b>33</b>

## FIGURES

	Page
<b>Figure 1. Stratigraphic variation of surface area for the Newbury samples</b>	<b>34</b>
<b>Figure 2. Downhole variation of surface area for the Jubilee Line Extension BH 404T</b>	<b>35</b>
<b>Figure 3. Stratigraphic variation of surface area for the Alum Bay</b>	<b>36</b>

## PLATES

	Page
<b>Plate 1: Typical example of Thanet Sand Formation, comprising well sorted fine grained sand, locally weakly cemented by detrital clay. Note oversized secondary voids due to feldspar dissolution. Sample JLE 52.80 m, Jubilee Line Extension BH 404T. (D789P1/01)</b>	<b>37</b>
<b>Plate 2: Typical view of moderately sorted, glauconitic sandy clay of the Upnor Formation in London Basin. Sample NB3, Newbury Bypass, 1.55-1.8m above Chalk (E439S1/03).</b>	<b>37</b>
<b>Plate 3: Internal fine-grained texture of a glauconitic sand grain in the Upnor Formation, London Basin. Sample NB3, Newbury Bypass, 1.55-1.8m above Chalk (E439S1/02).</b>	<b>38</b>
<b>Plate 4: Compacted detrital clay matrix with no lamination from the Upnor Formation in the London Basin. Sample NB3, Newbury Bypass, 1.55-1.8m above Chalk (E439S1/04).</b>	<b>38</b>
<b>Plate 5: Compacted detrital clay matrix with a weakly developed laminated fabric in the Upnor Formation, London Basin. Sample NB3, Newbury Bypass, site G, 1.55-1.8m above Chalk (E431S1/03).</b>	<b>39</b>
<b>Plate 6: Open root channel with clay particles oriented around channel wall. Sample NB3, Newbury Bypass, site G, 1.55-1.8m above Chalk (E431S1/04).</b>	<b>39</b>
<b>Plate 7: Detailed view of very weakly developed alignment of clay particles in the Upnor Formation, London Basin. Orsett Quarry, OQ2 (E435S1/03).</b>	<b>40</b>
<b>Plate 8: Detailed view of moderately developed alignment of clay particles in the Upnor Formation, London Basin. Orsett Quarry, OQ1 (E434S1/02).</b>	<b>40</b>
<b>Plate 9: Root channel filled by well sorted clean sand grains in the Upnor Formation, London Basin. Orsett Quarry, OQ1 (E434S1/04).</b>	<b>41</b>
<b>Plate 10: Poorly cemented, fine grained, glauconitic sand from the base of the Upnor Formation in Jubilee Line Extension BH 404T (40.35 m). Glauconite grains are light grey, quartz grains are mid grey with the enclosing clay matrix and clay laminae dark grey. Note the open pore network. (D785P1/01)</b>	<b>41</b>
<b>Plate 11: Glauconitic sand with clay laminae from the Upnor Formation in Jubilee Borehole 404T (38.01 m depth). Note the open porosity in the sandy areas and reduced porosity in the clay lenses. (D784P1/06)</b>	<b>42</b>
<b>Plate 12: Typical detailed view of glauconitic sand from the Upnor Formation in Jubilee Borehole 404T (38.01 m depth). Note corroded albite grain, angular quartz grains and glauconite grain (right) with pores lined by smectitic clay. (D784P1/03)</b>	<b>42</b>

- Plate 13: Glauconite pellet containing a calcium phosphate (collophane or apatite?) from the Upnor Formation in Jubilee Line Extension BH 404T (38.01 m depth). The extensive cracking may be due to drying. (D784P1/04)** 43
- Plate 14: Example of the clay-rich glauconitic sands from the Upnor Formation. Note oxidised glauconite grains and secondary porosity (much of which is thought to be drying artifacts prior to specimen preparation). Jubilee Line Extension BH 404T (36.30 m depth). (D783P1/02)** 43
- Plate 15: Example of the sandy clay from the upper part of the Upnor Formation with iron oxyhydroxide staining (light grey areas on right half of image) accounting for the yellow staining seen in hand specimen. Up is from right to left. Jubilee Line Extension BH 404T (35.40 m depth). (D780P1/01)** 44
- Plate 16: Detail of calcite concretions in the sandy clay from the upper part of the Upnor Formation. Up is from right to left. Jubilee Line Extension BH 404T (35.60 m depth). (D781P1/03)** 44
- Plate 17: Pyrite and calcite concretion in the upper part of the Upnor Formation possibly replacing the original clay matrix. Note that quartz grains have been fractured and then sealed by the pyrite. Jubilee Line Extension BH 404T (35.60 m depth). (D781P1/01)** 45
- Plate 18: Typical example of a sandy clay from the Reading Formation in the London Basin comprising detrital fine sand-sized grains in a clay matrix consisting of (in this example) major illite and kaolinite with minor smectite. Sample NB16, Newbury Bypass Site E, 19.7 m above Chalk. (E442S1/03)** 45
- Plate 19: Corroded K-feldspar in the Reading Formation of the London Basin. Sample NB16, Newbury Bypass Site E, 19.7 m above Chalk. (E442S1/01)** 46
- Plate 20: Clay matrix in the Reading Formation of the London Basin, in which the clay minerals (here major smectite with minor kaolinite and illite) occur in silt-sized aggregates. Note the relatively open porosity compared to plates 15 and 16. Sample NB1, Newbury Bypass Site A, 2.25 above Chalk m. (E438S1/07)** 46
- Plate 21: Detailed view of randomly oriented ragged clay flakes (here major smectite, minor illite and kaolinite) in the Reading Formation of the London Basin. Sample NB27C, Newbury Bypass 13.6 m above Chalk. (E443S1/04)** 47
- Plate 22: Example of a very weakly developed laminated sedimentary fabric in the Reading Formation of the London Basin. Sample NB7, Newbury Bypass 5.35 m above Chalk. (E440S1/02)** 47
- Plate 23: A rare well developed kaolinite book within the clay matrix of the Reading Formation of the London Basin. Sample M40. (E444S1/03)** 48
- Plate 24: Fine grained iron oxyhydroxide lining large void in Reading Formation of the London Basin. Sample NB1, Newbury Bypass 2.25 m above Chalk. (E438S1/05)** 48
- Plate 25: Detailed view of iron oxyhydroxide lining large void in Reading Formation of the London Basin. Sample NB1, Newbury Bypass 2.25 m above Chalk. (E438S1/03)** 49
- Plate 26: Irregular, micron-scale silica crystals forming a void lining in the Reading Formation of the London Basin. Sample NB16, Newbury Bypass Site E, 19.70 m above Chalk. (E442S1/02)** 49
- Plate 27: Typical view of blue-grey clay from the Upper Mottled Clay of the Reading Formation in the London Basin. Sample JLE26.3 m, Jubilee Line Extension borehole 404T. (D501/01)** 50
- Plate 28: Heavily altered clay from the Lower Mottled Clay in the Reading Formation in the London Basin. The original clay has been patchily altered to leave a siliceous matrix (dark grey area) and pervasively stained by iron oxyhydroxide (light grey). Expansive calcite rhombs (mid grey) form concretions throughout. Sample JLE 34.20 , Jubilee Line Extension BH 404T. (D777P1/01)** 50

<b>Plate 29: Detail of clay which has been altered to a siliceous matrix. Note the void is lined by colloform silica and subsequently by iron oxyhydroxide. Sample JLE 34.20 , Jubilee Line Extension BH 404T. (D777P1/03)</b>	<b>51</b>
<b>Plate 30: A calcite concretion and extensive precipitation of calcite rhombs within the clay. Note enclosed iron oxyhydroxide. Sample JLE 34.20 , Jubilee Line Extension BH 404T. (D777P1/06)</b>	<b>51</b>
<b>Plate 31: Sand-rich clay laminae in the Laminated Sands and Silts of the Woolwich Formation. Note corroded feldspars and splayed mica. Sample JLE 30.05 m , Jubilee Line Extension BH 404T. (D772P1/02)</b>	<b>52</b>
<b>Plate 32: Clay, sandy-clay and sand laminae in the Laminated Sands and Silts of the Woolwich Formation. Note variable porosity. Sample JLE 30.05 m , Jubilee Line Extension BH 404T. (D772P1/01)</b>	<b>52</b>
<b>Plate 33: Typical view of clay matrix, comprising major illite with minor kaolinite and smectite in the Upnor Formation from Alum Bay, Isle of Wight (6.0 m above Chalk). (D816S1/01)</b>	<b>53</b>
<b>Plate 34: Rare, coarse corroded kaolinite book in the Reading Formation of the Hampshire Basin in Alum Bay, Isle of Wight (17.6 m above Chalk). (D821S1/03)</b>	<b>53</b>
<b>Plate 35: Anhedral to occasionally micro-botryoidal goethite lining voids in the Reading Formation of the Hampshire Basin in Alum Bay, Isle of Wight (17.6 m above Chalk). (D821S1/06)</b>	<b>54</b>
<b>Plate 36: Hematite rosettes forming thin linings on voids in the Reading Formation of the Hampshire Basin in Alum Bay, Isle of Wight (18.9 m above Chalk). (D822S1/04)</b>	<b>54</b>

**British Geological Survey**

**Mineralogy and Petrology Report No. WG/98/4R**

**THE MINERALOGY AND PETROGRAPHY OF THE LAMBETH GROUP FROM  
THE LONDON AND HAMPSHIRE BASINS**

**J M Pearce, S J Kemp and V L Hards**

**1. INTRODUCTION**

The upper Palaeocene Lambeth Group (56-55 Ma) is widespread over the London and Hampshire Basins of southeast England. It comprises the Upnor Formation, which is overlain by the Reading Formation and Woolwich Formation. The lithostratigraphy and tectonic history of the Palaeocene in the southeast of England has been described in detail elsewhere (Ellison et al., 1994, 1996; Knox, 1996). A brief overview is provided here, largely based on these accounts. The Upnor Formation rests unconformably on the Thanet Sand Formation in the east of the London Basin but oversteps onto the Chalk in the west. Two facies have been recognised in the Upnor Formation. A lower glauconitic, calcareous pebbly sandstone with a shallow marine microfauna. In the London Basin glauconite can comprise 25 % of the sediment, resulting in a variably green colour. The upper facies comprises non-calcareous glauconitic sandstones and conglomerates, some of which contain silica-cemented pebbles. The more restricted microfauna and silica-cemented pebbles suggests a continental depositional environment, related to that of the overlying Reading Formation.

The Upnor Formation is overlain by the Reading Formation and the Woolwich Formation (see below). The Reading Formation comprises mottled clays, varying from red to blue-grey in colour due to pedogenesis. The proportion of sand varies but generally increases towards the base. The Reading Formation occurs in the north and west of the London Basin and interdigitates in east and central London with the Woolwich Formation. In the east the Reading Formation passes laterally into the Woolwich Formation.

The Woolwich Formation consists predominantly of grey to grey-brown, interlaminated fine-grained sands, silts and clays. Plant debris is common, concentrated in thin allochthonous lignites. Burrows are sporadic throughout, and bioturbation occurs towards the top of the formation. Shelly beds comprise brackish water shells in a clay matrix. In addition to overlying the Upnor Formation, the Woolwich Formation also overlies and interdigitates with the Reading Formation (see Ellison et al., 1996, Figure 3.). The Reading Formation and Woolwich Formations are overlain by the glauconitic sands and sandy clays of the Harwich Formation.

The Lambeth Group represents the middle of three depositional sequences. Below the Lambeth Group, the Ormesby Clay and Thanet Sand Formations represent deposition in outer muddy shelf and inner sandy shelf environments respectively (Knox, 1996). The Lambeth Group represents deposition in initially shallow marine to lagoonal facies (Upnor Formation), followed by nearshore marine to lagoonal (Woolwich Formation) and continental facies (Reading Formation). The overlying Thames Group, comprising the Harwich and London Clay Formations, marks a return to shallow marine conditions with the London Clay representing a further increase in sea level.

Following the regression and subaerial exposure, the Upnor Formation was deposited on the eroded Thanet Sand Formation, during a transgressive period from lagoonal to shallow open marine conditions with reconnection to the Atlantic indicated by nannoplankton assemblages. In the west, the glauconitic sands of the upper part of the Upnor Formation mark a sea-level fall and return to restricted shallow marine to lagoonal conditions. In the east, the upper part of the Upnor Formation sands and conglomerates represent deposition in a littoral to sublittoral environment. The pollen and spore assemblages indicate that the hinterland to the Upnor Formation contained extensive wet lowland areas. With continued uplift in the west, the lower Reading Formation was deposited in continental conditions along the margin of the Anglo-Paris Basin with the relative uplift of the source areas in the west keeping pace with increasing sea-levels and resulting in deposition of continental clastic sediments. This more local provenance for the Lambeth Group sediments is in marked contrast to the Scottish provenance of the Thanet Sand and Harwich Sand below and above (Morton, 1982).



The continental conditions of the Reading Formation led to extensive pedogenesis of the upper parts of the Upnor Formation and much of the Reading Formation. In the Upnor Formation this resulted in the development of carbonate concretions, clay enrichment and colour mottling. In the Reading Formation the extensive mottling is due to pedogenesis in the humid conditions (Buurman, 1980). The mottling was caused by the alternating reducing and oxidising conditions, within the zone between low and high groundwater levels, which caused segregation of iron and manganese compounds. The colour of the iron segregations depends on the degree of hydration: strongly hydrated iron oxyhydroxides are yellow (XRD analyses in this study indicate this is likely to be goethite, lepidocrocite and jarosite) and turn progressively redder with dehydration (XRD analyses in this study indicate this was likely to be predominantly hematite). Following sedimentation, emergence and drying, possibly with the establishment of a vegetative cover, the cycle of reducing and oxidising conditions was initiated by the development of dense clay accumulations following clay mobilisation and illuviation. Reducing conditions were developed following stagnation of pluvial water above these impermeable clay layers. Pyrite was precipitated in former root holes and voids rich in organic matter. Pyrite was then subsequently oxidised during the next phase of emergence or during later tectonic uplift to produce the varied mottling described above.

This report presents results of an extensive mineralogical and petrographical study of the Lambeth Group and a very brief examination of three samples from the underlying Thanet Sand Formation. Particular emphasis was placed on those characteristics of the samples which most influence the engineering properties. These are strongly influenced by the proportions and mineralogy of the clay minerals, especially swelling clays such as smectite, the nature of open porosity and distribution of iron oxyhydroxide minerals.

## **2. SAMPLES**

A total of 95 samples of clays and sands from the Lambeth Group were analysed by X-ray diffraction (XRD) and surface area determination techniques. The samples were submitted in three batches. The first batch (39 samples) were collected from the Upnor and Reading Formations from the Newbury Bypass area, Berkshire, the Upnor Quarry, Kent and the Orset Quarry, Essex (Table 1). The second batch (40 samples) was taken from Alum Bay, Isle of Wight, Hampshire together with a selection of other localities including quarries and clay pits

(Table 3). The third batch contained 16 samples from the Jubilee Line Extension BH 404T for surface area analyses only (Table 2). Sample details, including localities and brief lithological descriptions, are given in Tables 1, 2 and 3.

A subset of the samples examined by XRD were also studied petrographically by scanning electron microscope (SEM). A total of 30 samples were examined; 17 samples by secondary electron SEM and 13 polished thin sections prepared from samples taken from the Jubilee Line Extension borehole were examined by backscatter SEM.

### **3. LABORATORY METHODS**

#### **3.1. X-ray diffraction (XRD) analysis**

The samples were supplied in field-moist condition, and a representative portion of each was first dried in an oven at 55 °C while the remainder was retained for reference purposes. The dried clays were then jaw-crushed, and a further sub-sample of this material (~10 g) hammer-milled pass a 125 µm screen. The unconsolidated nature of the sand samples meant that hammer-milling only was required. In order to produce a finer and uniform particle-size for whole rock (bulk) XRD analysis, representative sub-samples of the hammer-milled materials (~3 g) were micronised under acetone for five minutes and dried at 55 °C before being back-loaded into standard aluminium sample holders.

In order to study any clay minerals present in the samples, fine (<2 µm) fraction oriented mounts were prepared. Representative sub-samples (~10 g clays or 25 g sands) of the jaw-crushed materials were further crushed to <2 mm in a pestle and mortar. The <2 mm material was then dispersed in 150 ml of deionised water by sloughing, shaking for 2 hours on a reciprocal shaker and treatment with ultrasound for approximately 3 minutes. The resultant suspensions were then sieved on 63 µm and the <63 µm fractions placed in 250 ml measuring cylinders and allowed to stand. To prevent flocculation 1 ml of 0.1 M Calgon (sodium hexametaphosphate) was added to each of the suspensions. After a period dictated by Stokes Law, nominal <2 µm fractions were removed and dried at 55 °C. 100 mg of each of the <2 µm materials was then re-suspended in a minimal amount of distilled water and pipetted onto a ceramic tile in a vacuum apparatus to produce an oriented mount. The mounts were

Ca-saturated using 2 ml of 1 M  $\text{CaCl}_2 \cdot 6\text{H}_2\text{O}$  solution, washed twice to remove excess reagent before being allowed to air dry.

XRD analysis was carried out using a Phillips PW1700 series diffractometer using  $\text{Co-K}\alpha$  radiation and operating at 45 kV and 40 mA. For bulk analysis the micronised powder mounts were scanned over the range 3-50  $^\circ 2\theta$  at a scanning speed of 0.52  $^\circ 2\theta/\text{minute}$ . The oriented mounts were scanned over the range 1.5-32  $^\circ 2\theta$  in both air-dried and ethylene glycol-solvated states, and after heating to 550  $^\circ\text{C}$  for 2 hours. Diffraction data were analysed using Phillips APD1700 software coupled to an International Centre for Diffraction Data (ICDD) database running on a DEC Micro Vax 2000 micro-computer system.

### **3.2. Scanning electron microscopy (SEM) analysis**

A small subsample was carefully split from the field-moist samples and freeze-dried. This involves initial pre-freezing in liquid nitrogen. The rapid freezing allows pore waters to form ice glass and prevents the growth of ice crystals which develop at slower cooling rates. The formation of ice crystals would be disruptive to the fabric and might damage delicate clay morphologies. The frozen subsamples were then dried under vacuum for approximately 24 hours in an Edwards Modulyo freeze drier, in which the ice is sublimed. The dried subsamples were then mounted on aluminium pin-type stubs using a graphite carbon cement and coated in a thin layer of carbon, approximately 25 nm thick by evaporation in an Emitech evaporation coater.

The subsamples for polished thin section were initially impregnated with an epoxy blue-dyed resin. Thin sections were then cut and polished to a submicron finish, before coating in a thin layer of carbon as per the stubs.

All specimens were examined in a Leo 435VP SEM fitted with a four element solid-state backscattered electron detector. An Oxford Instruments Isis 300 energy-dispersive X-ray microanalysis (EDXA) instrument allowed routine mineral identification.

### **3.3. Surface area determination**

Surface area determinations were performed on all samples excluding the seven sands/sandy clays (samples NB4, NB5, NB9, NB10, NB20, NB26 and OQ3). The surface area of the samples was determined using the 2-ethoxyethanol (ethylene glycol monoethyl ether, EGME) technique. The method is based on the formation of a monolayer of EGME molecules on the clay surface under vacuum. Aluminium dishes containing approximately 1.1 g hammer-milled sample/clay standard (Patterson Court Blue Bentonite - the control) were firstly placed in a desiccator containing anhydrous phosphorus pentoxide, evacuated, and allowed to stand before being accurately weighed. Samples were then saturated with EGME and placed in a second desiccator containing dry calcium chloride. After one and a half hours the desiccator was evacuated and left over night. The sample was then rapidly re-weighed and the weight of the EGME absorbed determined and the surface area calculated. A correction, based on the control, was applied for slight variations between runs.

Smectite has a surface area of 800 m<sup>2</sup>/g while other clay minerals and quartz have surface areas typically less than 40 m<sup>2</sup>/g and 1 m<sup>2</sup>/g respectively. Such a difference in value means that the surface area of a sample can provide a useful estimate of its smectite content.

## **4. RESULTS**

### **4.1. Summary of mineralogy**

The results of both bulk and clay (<2 µm) fraction XRD analysis are summarised in Tables 4 to 8. The results of surface area determinations and equivalent smectite concentrations, based on a standard smectite surface area of 800 m<sup>2</sup>/g, are also given in Tables 4 to 6.

The whole-rock compositions of the clays are dominated by quartz and smectite, with minor-trace amounts of kaolinite, undifferentiated mica species, feldspars, iron oxides (goethite, lepidocrocite and hematite), pyrite and jarosite. The sands are predominantly composed of quartz, with minor amounts of feldspar (K-feldspar and albite) and clay minerals.

The clay mineral assemblages of the samples are composed of varying proportions of smectite, illite and kaolinite. The <2 µm fractions also contain significant quantities of the iron oxyhydroxides lepidocrocite and goethite.

## **4.2. The London Basin**

### **4.2.1. Thanet Sands**

Polished thin sections of three samples (JLE 47.0 m, JLE 48.01 m and JLE 52.80 m) of the Thanet Sand Formation from the Jubilee Line Extension borehole 404T were briefly examined. All three samples are very similar comprising very well sorted, fine grained sands (Plate 1). The sands are largely very poorly cemented in thin section with minor detrital clay forming irregular patches up to a few millimetres across in some areas (Plate 1). The sand consisted predominantly of angular to subangular quartz grains with minor K-feldspar, mica, chlorite and ilmenite grains, and rare glauconitic grains. In such well sorted sands with minimal clay matrix primary porosities are very high and have been locally further enhanced by dissolution and corrosion of feldspar grains (Plate 1). Rare authigenic pyrite is occasionally developed but does not form a significant cementing phase.

### **4.2.2. The Upnor Formation**

Samples from the Upnor Formation, represented by four samples from Newbury (NB18, NB19, NB3 and NB4) and the samples from Orsett and Upnor quarries, have a non-clay mineralogy predominantly composed of quartz with minor-trace quantities of K-feldspar, albite, mica, goethite and hematite. Clay mineral assemblages are again dominated by smectite with minor quantities of illite and kaolinite. Exceptionally, the clay mineralogy of sandy clay sample UQ3 is dominated by kaolinite with only traces of smectite and illite. Surface areas indicate equivalent whole-rock smectite contents in the range 3 to 41 % (mean = 18 %).

SEM analysis of Upnor Formation samples NB3 (E439) and NB18 (E431) from the Newbury Bypass site indicate that they are sandy clays (Plate 2). The sand grains are moderately sorted and vary from very fine to medium sand with occasional coarse sand-sized grains. The modal grain size, based on a visual inspection only, is estimated to be fine sand. The sand grains are generally well rounded, equant, subspherical and float in the clay matrix. In addition to the non-clay mineralogy described above, sand-sized rounded glauconite grains

are also present and have a typical fine-grained internal texture (Plate 3). Occasional quartz and K-feldspar grains are corroded. The smectite-dominated clay matrix comprises ragged irregular particles which form more massive structureless clay in some areas. EDXA indicates a K, minor Mg, Fe aluminium silicate chemistry. Sample NB3 (Plate 4) is more compacted than sample NB18 which has a more open texture (Plate 5). Within the clay matrix, porosity is generally low, being restricted to interparticulate submicron voids. The clay fabric shows poor to moderate alignment of clay flakes producing weak laminations. Disruption of the primary sedimentary fabric leads to adjacent discrete areas of laminated clay having different orientations. From the limited evidence obtainable by SEM, the cause of this disruption is not clear; soft-sediment reworking, bioturbation and pedogenesis are possibilities (see Section 5.3 for discussion about the origin of the clay minerals). Open, unfilled root channels around which clay particles are oriented (Plate 6) provides evidence for subaerial exposure and pedogenesis.

Two samples of the Upnor Formation were examined from Orsett Quarry, OQ1 (E434) and OQ2 (E435). These samples of the Upnor Formation differs slightly from those at the Newbury Bypass site. Here they are silty clays with a significantly reduced proportion of silt and sand grade material. The silt-sized detrital grains are typically subrounded to subangular. Rare K-feldspar grains are typically corroded. Although the clay particles show variable, weak to moderate alignment through compaction on the SEM scale (Plates 7 and 8), there is only a weakly developed lamination at the hand specimen scale. The clay particles themselves are very small, typically submicron, but have combined to form larger aggregate particles up to 5  $\mu\text{m}$  maximum size (Plates 7 and 8). EDXA again indicates the smectite-rich clay is an intergrowth of smectite and minor illite on the scale of the electron beam interaction volume (1-2  $\mu\text{m}^3$ ). Although detected by XRD in both the whole rock and clay fractions and by EDXA, no discrete kaolinite particles were observed, indicating that the clay minerals are finely intergrown at a scale too small to be resolved by SEM. A root channel present in one sample (OQ1) has been filled by well sorted, coarse, subrounded to subangular, clean sand grains (Plate 9). As noted in the Newbury Bypass samples, some of these sand grains are slightly etched.

Six samples of the Upnor Formation glauconitic sand from the Jubilee Line Extension borehole 404T were examined, 35.40 m, 35.6 m, 36.25 m, 38.01 m, 38.01 m and 40.35 m.

The deepest sample examined (40.35 m) comprises a very loosely cemented, moderately to well sorted, fine sand (Plate 10). The detrital grains consist predominantly of subangular to subrounded quartz with minor K-feldspar and glauconite grains plus trace mica. Occasional irregular and intermittent clay lenses and discrete patches of detrital clay locally weakly cement the sand (Plate 10). The low proportion of clay matrix and absence of authigenic cements result in a very high primary intergranular porosity which has been significantly enhanced by considerable framework grain dissolution (Plate 10), particularly of feldspars. The rare micas are altered with consequent splaying along basal cleavage planes. This sample is very similar to the underlying Thanet Sand Formation (Plate 1), the top of which is 0.78 m below this sample.

The sample at 38.01 m in the borehole is a moderately sorted, mainly sub-rounded to rounded, medium-grained sand (Plate 11). It consists predominantly of quartz with minor K-feldspar and glauconite, and trace amounts of flint grains, plagioclase and mica. The flints, plagioclase and K-feldspar are corroded, producing oversized secondary voids (Plate 12). Detrital smectitic clay lines many of the primary and secondary voids. The glauconite grains are typically rounded but are generally slightly coarser than the sand grains. The glauconite grains are occasionally concentrated in certain laminae with adjacent sand laminae containing fewer glauconite grains. They occasionally contain patches of fine grained calcium phosphate (Plate 13) which appears to have grown expansively to enclose fragments of the glauconite. The phosphatic material, possibly apatite or collophane, appear to have formed after the glauconite pellet during early diagenesis. Compaction has led to some of the glauconite grains being deformed around the other detrital sand grains.

Clay laminae, lenses and pockets occur throughout and enclose the detrital sand grains (Plate 11). In the clay laminae porosity is very low. In the sands the porosity forms an open, well connected network. However, permeability is reduced by detrital clay coatings around many grains which block many pore throats and act as a weak cement (Plate 12). The similar chemistry of the clay coatings to those present in other parts of the London basin described above indicates that it is likely to be comprised of a similar mixture of smectite, illite and kaolinite. XRD analysis of the Upnor Formation (Knox, 1997) determined the clay matrix (<4 µm fraction) contained dominant smectite with minor but variable amounts of illite,

chlorite and kaolinite. Rare euhedral iron-rich carbonate crystals, <10 µm across, possibly ankerite or siderite, occur in voids.

The samples at 36.25 m and 36.30 m are very similar comprising clay-rich sands. The sand component consists predominantly of angular to subrounded, equant to irregular, moderately sorted, detrital quartz grains (Plate 14). Minor components are rounded glauconite grains and K-feldspars. The sand has a grain- to matrix-supported fabric with clay filling intergranular voids and also forming more extensive areas of clay (Plate 14). Knox (1997) determined the clay mineralogy of the <4 µm fraction over this interval to be dominated by smectite (~ 90 %) with minor illite and smaller amounts of chlorite and kaolinite. Minor compaction has led to some deformation of the glauconite pellets around quartz grains. The primary porosity is infilled by abundant clay matrix and most of the porosity visible in the thin sections is thought to be an artefact of sample drying prior to specimen preparation. Secondary porosity has developed due to corrosion of feldspar grains and feldspar in rare lithic fragments. Many of the glauconite grains are partially to extensively replaced by iron oxyhydroxide.

The uppermost two samples examined (35.40 m and 35.6 m) are sandy clays. EDXA indicates that the matrix may contain significant amounts of glauconitic clay although XRD analysis of the <4 µm fraction indicated that the matrix comprised major smectite (~80-90 %) with minor illite, chlorite and kaolinite. Moderately sorted, angular to well rounded, medium grained quartz grains with minor rounded glauconite grains and, often corroded, feldspar grains plus rare micas and porous flints are supported by this clay matrix (Plate 15). The yellow mottling seen in hand specimen is due to extensive iron oxyhydroxide staining and replacement of the clay matrix (Plate 15). The staining occurs in discrete irregular patches on a millimetre-scale throughout the specimens.

The carbonate patches at 35.6 m recognised in hand specimen consist of anhedral to subhedral calcite crystals varying in size from submicron to 20 µm in diameter (Plate 16), which form replacive and/or expansive patches up to several millimetres across within the clay matrix. These patches enclose isolated sand grains and have well defined boundaries with the enclosing clay matrix. Pyrite is associated with these calcite concretions, forming the dominant component in some cases (Plate 17). Networks of anastomosing cracks through quartz sand grains are sealed by the enclosing pyrite (Plate 17).



Variations in surface area measurements are generally attributable to the variations in proportion of clay. Figure 1 shows a plot of surface area against depth above the Chalk for the Newbury samples. Surface area values show an overall decrease with increasing distance from the top of the Chalk with the highest value occurring in the lowermost sample in the Upnor Formation. A similar decrease in surface area with increasing distance from the Chalk was also noted for the Orsett and Upnor Quarry samples.

#### 4.2.3. The Reading Formation

The Reading Formation samples from the London Basin, represented by samples from Newbury, Copyhold and Hermitage Farms, the M40 section, Chievely Pit, Glazenwood and Enfield, present non-clay mineralogies composed of varying proportions of quartz, feldspar, mica, hematite, goethite and lepidocrocite. Clay mineralogies are predominantly composed of smectite with subordinate quantities of illite and kaolinite. Equivalent smectite contents derived from surface area data range from 1 to 34 % (mean = 20 %). No clear trends in the smectite content are apparent but generally they reflect the quantity of clay present i.e. high values in the clays and lower values where significant amounts of sand-grade material is present.

Five samples of sandy clays (Plate 18) from the Reading Formation at the Newbury Bypass site (NB1, NB7, NB15, NB16 and NB27C) and one from the M40 site in the London basin were examined by SEM. The sand grains are predominantly rounded, fine sand-sized to silt-sized quartz grains with rare feldspar grains. The feldspars are typically corroded to varying degrees, occasionally with extensive corrosion leading to relict skeletal grains (Plate 19). These grains largely float in a clay matrix of variable texture.

In three of the samples examined, NB1, NB15 and NB16, the clay matrix consists largely of an apparently structureless intergrowths, i.e. individual clay particles are too small to be resolved by SEM. This very fine-grained clay forms aggregate particles of up to silt size (Plate 20). These samples suggest a more open pore network than the others examined due to the clay fabric largely being made up of discrete silt-sized clay aggregates. Occasionally, however, the aggregate clay particles have poorly developed flaky morphologies.

In the other two samples examined, NB7 and NB27C, the clay matrix consists of irregular, ragged detrital clay flakes. In most areas these clay flakes are more or less randomly oriented (Plate 21). However, in limited areas of some samples a weakly laminated sedimentary fabric (Plate 22), developed through compaction, has been preserved. In these samples the porosity appears to be much lower and the weak lamination will reduce permeability accordingly. However, the differences observed petrographically are not reflected in the mineralogy of the <2 µm fractions which show no systematic differences except in the iron oxyhydroxides (see below).

Some surfaces are slightly polished indicating that these are slip surfaces. A poorly developed hexagonal ridge of ?smectitic clay occurs on many of these surfaces. This is likely to be a drying artefact from possible clay suspensions along the slip planes.

XRD indicates that kaolinite is present in all samples analysed from the Reading Formation at the Newbury Bypass site. However, it generally occurs intimately associated with the smectite and illite within the matrix and is therefore not easily resolved. Moderately to well developed kaolinite books occur only rarely as isolated particles up to 20 µm across in the Newbury Bypass samples but are better developed in the sample from the M40 site (Plate 23). Iron oxyhydroxides are common in all samples with goethite being detected by XRD and lepidocrocite detected in samples NB7 and NB27C. EDXA typically detects relatively high iron concentrations in many qualitative analyses of the clay matrix indicating that most of the iron oxyhydroxides are intimately associated with the clay minerals. However, in samples NB1 and NB27C, discrete well developed fine grained iron oxyhydroxide occurs lining relatively large voids up to at least 100 µm across (Plate 24). In detail, the iron oxyhydroxide forms submicron-size, equant platelets (Plate 25). EDXA indicates the iron oxyhydroxide is associated with kaolinite and occasional poorly developed kaolinite books develop within these void linings. In addition to the iron oxyhydroxides, EDXA also detected relatively high silicon concentrations in many areas of the clay matrix. It is also associated with the iron oxyhydroxide void linings. Again this probably indicates the presence of a silica phase intimately associated with these minerals. The lack of any evidence from XRD of a silica phase would suggest that it may be X-ray amorphous. However, it may occur at concentrations below XRD detection limits or diagnostic peaks

may be obscured by those of other phases. Occasionally the silica develops as micron-scale irregular crystals lining voids (Plate 26).

BSEM analysis of two thin sections from the Upper Mottled Clay, Reading Formation, from the Jubilee Line Borehole 404T (26.3 m and 27.80 m), show very similar petrographic characteristics to the Newbury Bypass samples described above. These are silty clays comprising silt-sized detrital quartz, K-feldspar and occasionally deformed micas, and minor amounts of chlorite in a very fine grained clay matrix (Plate 27). Knox (1997) determined the clay mineralogy to be a mixture of approximately equal proportions of smectite, illite and chlorite plus approximately 10 % kaolinite. BSEM also indicates the presence of common titanium oxide specks and iron oxide specks throughout. Rare ferromagnesian minerals are altered to iron oxyhydroxides. Rare pyrite grains occur as isolated submicron cubes and occasionally as larger irregular crystals up to 40  $\mu\text{m}$  across. In some areas the micas depict very weakly developed lamination but, as seen in the Newbury Bypass samples, this is only poorly developed and restricted to discrete patches with adjacent areas having similarly developed weak alignments but in different orientations. The mottling observed in thin section is due to extensive iron staining of the clay matrix on all scales up to centimetres across. In thin section, the staining occurs as irregular patches with the outer boundaries having the highest iron oxyhydroxide concentrations. Iron oxyhydroxide also forms irregular millimetre-scale stringers, sometimes infilling irregular cracks in the clay matrix.

The sample examined by BSEM from the Lower Mottled Clay in the Reading Formation (34.20 m), generally has the same features as the sample from the Upper Mottled Clay. This sample is an extensively altered clay. Initially, the clay matrix was patchily altered to produce a siliceous cement extensively charged with iron oxyhydroxide (Plate 28). The silica also forms colloform linings around open voids which is subsequently coated in iron oxyhydroxide (Plate 29). As in the previous samples the iron oxyhydroxide forms a pervasive stain of varying intensity which is confined to irregular discrete millimetre-scale patches (Plate 28). Calcite forms subspherical concretions comprised of euhedral to subhedral rhombs up to 50  $\mu\text{m}$  in length (Plate 30). The clay matrix surrounding these concretions is also heavily charged with these rhombs. Iron oxyhydroxide is entrained within some of these concretions suggesting that the calcite precipitated after the iron oxyhydroxide. Calcite has precipitated with an expansive texture.

Figure 2 shows a stratigraphic downhole plot of surface area distribution for the Jubilee Line Extension BH 404T. The Lower Mottled Clays of the Reading Formation produced the highest surface areas in the borehole, equivalent to 33-48% smectite with the exception of the shallowest calcareous sample which has a lower value equivalent to 18% smectite. High surface area values are in agreement with the XRD clay mineralogy analyses produced by Knox (1997) which indicate a smectite-dominated clay mineralogy with only traces of illite, chlorite and kaolinite.

The Upper Mottled Clay of the Reading Formation show a return to moderate surface areas with a mean value equivalent to c.28% smectite. However, these represent lower surface area values than in the Lower Mottled Clay. The difference in surface area between the two intervals is due to the lower smectite and higher illite, chlorite and kaolinite concentrations in the Upper Mottled Clay relative to the Lower Mottled Clay. The silt/sand at the top of the Upper Mottled Clay has a very low smectite content of 2%.

#### 4.2.4. The Woolwich Formation

The two samples from the Woolwich Formation in the Upnor Quarry have a different non-clay mineralogy compared to the Reading and Upnor Formations. Although also predominantly composed of quartz, samples UQ4 and UQ5 contain minor-trace quantities of gypsum, aragonite, mica and possibly pyrite and goethite. Clay mineralogies, however, are similar to the Reading and Upnor Formations and are dominated by smectite with minor illite and kaolinite.

A polished thin section from the Laminated Sands and Silts of the Woolwich Formation, from the Jubilee Line Extension BH 404T (JLE 30.05 m), was examined by BSEM. This sample is a weakly laminated clay with common millimetre to centimetre-scale sand to silt lenses and laminae. The sand laminae consist of fine grained angular, predominantly poorly-sorted to occasionally well-sorted quartz with minor K-feldspar and mica, generally within a clay matrix (Plate 31). Trace amounts of heavy minerals are concentrated in the sandier laminae. Possibly authigenic titanium oxide (?anatase) occurs disseminated throughout the clay matrix. Feldspars are corroded and micas are altered with expansion along basal cleavages (Plate 31). XRD analysis (Knox, 1997) indicated that the clay matrix of the

Laminated Sands and Silts contains approximately 50-70 % smectite, 10-20 % illite, 3-10 % chlorite and 5-10 % kaolinite. Porosity is extremely variable in this sample (Plate 32). Although porosity is very low in the sand-free clay laminae, areas of sand and silt which contain a clay matrix have higher porosity. Some of the sandier lenses contain well developed open porosity and no clay matrix.

The sample from the Lower Shelly Clay of the Woolwich Formation has a moderate surface area, equivalent to 29% smectite, reflecting the decrease in smectite detected by Knox (1997). The single sand sample from the overlying Laminated Sands and Silts of the Woolwich Formation, unsurprisingly shows a further decrease in surface area equivalent to 16% smectite.

Surface area determinations from the Upper Shelly Clay of the Woolwich Formation indicate low smectite contents of <14 %. XRD analyses, however, suggest a higher smectite content than in the underlying Upper Mottled Clay.

### **4.3. Summary of mineralogy and petrography in the London Basin**

#### **4.3.1. Upnor Formation**

The Upnor Formation in the London Basin comprises interlayered glauconitic clay-rich sands and clays. Glauconite typically forms during early diagenesis in shallow marine conditions and previous studies indicate these sands were deposited during transgressive periods in a shallow marine environment (Ellison et al., 1994; Knox, 1996). The sands comprise generally moderately to well-sorted fine to medium, subangular to rounded quartz grains in a clay matrix. Rare feldspar grains and flints are often at least partially corroded. The clay matrix consists of intergrowths of predominant smectite and minor kaolinite and illite which form up to silt-sized particles. Limited compaction has resulted in slight deformation of some glauconite grains around detrital quartz. Porosity varies between open pore networks in the sands to very low porosity in the clay laminae and clay-rich sands. Permeability is likely to be restricted in the sands by clay coatings which may partially block pore throats. Glauconite grains are partially oxidised and replaced by iron oxyhydroxide. Iron oxyhydroxide also patchily replaces the clay matrix. Pyrite and calcite form replace and possibly expansive concretions within the sands. The presence of iron oxyhydroxide, pyrite and calcite indicates fluctuating redox conditions while the presence of open and filled root channels indicates a

pedogenic environment. It is possible (although no direct evidence was observed) that the iron oxyhydroxide staining represents oxidation and remobilisation of reduced iron-bearing phases such as glauconite and pyrite.

#### 4.3.2. Reading Formation

The Upper and Lower Mottled Clays of the Reading Formation comprise sandy to silty clays. The non-clay grade material comprises predominant subangular to subrounded quartz with minor, generally corroded feldspars. The clay matrix in most samples is dominated by smectite with minor intergrown kaolinite and illite. However, kaolinite is the dominant mineral in some clay assemblages. The clays show no or a very weakly developed lamination in most samples. Kaolinite also occurs as rare, isolated moderately developed books. The primary mineralogy is subsequently modified by iron oxyhydroxide staining which produces the mottling and is the result of variable redox conditions in an intermittently saturated soil. Precipitation of silica patchily replaces the clay matrix and lines some voids.

#### 4.3.3. Woolwich Formation

The Laminated Sands and Silts of the Woolwich Formation consist of a weakly laminated clay with common millimetre to centimetre-scale sandy lenses. The clay matrix comprises predominant smectite with minor illite, chlorite and kaolinite.

### 4.4. The Hampshire Basin

The clay samples from the Alum Bay section have a non-clay mineralogy composed of major amounts of quartz with minor-trace quantities of mica, goethite, albite, K-feldspar and hematite. Their clay mineral assemblages are typically dominated by kaolinite with minor-trace quantities of illite, smectite and occasional chlorite. Exceptionally, the samples at 7.6 m and 18.9 m above the Chalk are dominated by illite and smectite respectively. Goethite forms a significant component of the <2  $\mu\text{m}$  material in the Alum Bay samples. Figure 3 shows a surface area distribution plot for the Alum Bay samples plotted against depth above the top of the Chalk. As for the London Basin samples, the variations in surface area appear to be proportional to the different sand, silt and clay contents.

One sample, from 0.3 m above the Chalk at Alum Bay on the Isle of Wight, was examined from the Upnor Formation of the Hampshire Basin by SEM. This sample is a poorly cemented, friable, clayey sand comprising predominantly generally angular to minor subrounded, moderately sorted quartz with rare corroded, blocky K-feldspar. The detrital sand grains are weakly cemented by a structureless clay matrix which XRD indicates is dominated by illite with minor amounts of kaolinite and smectite. No discrete authigenic kaolinite books are present, suggesting that these minerals are present intimately intergrown with the illite. Calcite occurs as millimetre-scale microporous laminae within the clay matrix, comprising predominantly anhedral to subhedral rhombs up to 10  $\mu\text{m}$  long. Iron oxides are occasionally poorly developed as irregular, fine grained flaky patches lining some voids. Porosity is generally low and is likely to have a low connectivity due to the abundant clay matrix which infills most voids and blocks pore throats.

Five samples of the Reading Formation (6.0 m, 7.6 m, 17.6 m, 18.9 m and 31.1 m above the Chalk) were examined from Alum Bay. The lowest sample from the Upnor Formation at Alum Bay (6.0 m above the Chalk) is a friable clay with abundant red iron oxyhydroxide spots. The clay is massive with no lamination developed. It comprises relatively large clay flakes up to 10  $\mu\text{m}$  across, at least some of which consist of intergrown major kaolinite with minor illite and smectite (Plate 33). Kaolinite plates can be observed occurring as rare isolated anhedral particles up to 5  $\mu\text{m}$  across. Domains of clay particles with common orientations form locally with adjacent domains having different orientations. Detrital quartz grains are very rare silt-grade clasts in this specimen. Although XRD indicates the presence of trace amounts of goethite, it is predominantly intimately intergrown with the clay particles and only very rarely is it resolved specifically lining small voids.

The second sample at 7.6 m is a friable clay with abundant red spots. The clay matrix comprises a series of domains within which the clay particles are randomly oriented. These domains are bounded by clay plates with a moderate alignment which forms a low-porosity coating around the domains. These moderately oriented areas do not develop a preferred orientation throughout the whole sample but form a three-dimensional network of channels around the domains. This texture suggests limited pedogenesis has taken place. Rare, poorly

developed goethite forms irregular linings on some voids, comprising submicron anhedral, vaguely flaky particles.

The samples at 17.0 m, 18.9 m and 31.1 m above the Chalk are silty to sandy clays containing common red spots. The clay matrices are very similar to the previous sample comprising intergrowths of major kaolinite with minor illite and smectite. The clay forms millimetre- to centimetre-scale domains, within which the clay particles are randomly oriented. The domain boundaries are marked by locally oriented clay particles which form non-porous coatings around the domains. As before, most of the kaolinite occurs intimately intergrown with the other clay minerals. However, kaolinite also occurs in these samples as rare, silt to sand-sized kaolinite books. These books tend to be moderately well developed euhedral particles some of which are corroded around their edges (Plate 34). At 31.1 m, authigenic submicron-scale irregular clay strands have developed.

The silt- to sand-sized detrital grains comprise major, angular to subrounded, moderately sorted quartz with trace amounts of corroded K-feldspar and albite. In some areas the sandy components are relatively clean with only a small amount of clay matrix infilling pores. Goethite develops as large patches (up to centimetre-scale in hand specimen) lining voids comprising micro-botryoidal to anhedral crystals (Plate 35). In addition to the goethite, patches of calcite and rare silica occur separately and comprise microporous, largely anhedral, micron-scale particles. The calcite occasionally also forms blocky, subangular to subhedral crystals. At 18.9 m, hematite forms large irregular patches up to centimetres across but only a few microns thick, lining voids within the clay. These patches comprise sub-micron plates in moderately developed rosettes (Plate 36).

The other Reading Formation samples from the Hampshire Basin (Knoll Manor, Michelmarsh and Whitecliff Bay) have a similar quartz, mica, feldspar, hematite and goethite non-clay mineralogy. Clay mineralogies are composed of various proportions of kaolinite, illite and smectite. The clay comprises submicron- to micron-scale intergrowths which form up to silt-sized particles. Both samples contain minor silt-sized irregular, angular quartz grains with rare K-feldspar and mica. The sample from Knoll Manor also contains rare poorly developed kaolinite books. These books are corroded leading to the development of oversized secondary voids in some cases.



The two Newhaven samples (Woolwich Formation) have a slightly different non-clay mineralogy as both samples contain pyrite and the sand also contains jarosite, a common product of pyrite weathering (Kemp and Pearce, 1992). Their clay mineralogies, however, are similar to the other Hampshire Basin samples.

#### **4.5. Summary of mineralogy and petrography in the Hampshire Basin**

##### **4.5.1. Upnor Formation**

The samples from the Upnor Formation in the Hampshire Basin comprise sandy clays and clays. The clay-grade material comprises intergrown smectite, kaolinite and illite in variable proportions. The clay matrix in the sands consists of dominant illite and in the clays contain dominant kaolinite. Goethite is also present intimately mixed with the clay particles. Some evidence exists for the clays having undergone limited pedogenesis with the development of domains containing randomly oriented particles, bounded by thin weakly aligned clay coatings.

##### **4.5.2. Reading Formation**

The Reading Formation in the Hampshire Basin comprises clays, sandy clays and clay-rich sands. The mineralogy is very similar to that observed in the London Basin with the clay matrix being dominated by kaolinite.

### **5. DISCUSSION**

#### **5.1. The London Basin**

Recent published data on the mineralogy of the Lambeth Group in the London Basin is relatively sparse. Most of the work was carried out in the 1960s and is summarised in Perrin (1971).

Weir and Catt (1969), in an investigation of the Palaeogene sediments of NE Kent showed that, in general, smectite is the dominant clay mineral with subordinate mica and kaolinite. Kaolinite, however, is absent from the lower part of the Woolwich Beds. Three sources of detritus were suggested: solution residues from the Chalk, the Armorican granitic province of

the southwest and a tract of metamorphic rocks. In their view, smectite was only partly derived from the Chalk although they are uncertain as to another detrital or authigenic origin.

The Reading Beds in the London Basin also contain assemblages dominated by smectite with minor kaolinite and mica. Gilkes (1966, 1968) considered this assemblage to be similar to that found in the Reading Beds of the eastern Hampshire Basin and suggested the Chalk to be the main source of smectite in that area. Avery et al. (1959) also recorded highly montmorillonitic clays from the Reading Beds from Harefield and Lane End, Buckinghamshire.

Bateman and Moffat (1987) studied the Woolwich and Reading Formation of the Chiltern Hills. The clay mineral assemblages were dominated by expansibles, particularly to the east, with minor kaolinite and mica, with the exception of the bottom bed where kaolinite was often more abundant.

Rae and Parker (1992) found samples of the Woolwich and Reading Beds to have a clay mineralogy dominated by a highly smectitic illite/smectite (I/S) with subordinate illite and kaolinite.

The samples from the present study have similar clay mineralogies that are predominantly composed of smectite with subordinate quantities of illite and kaolinite. Equivalent smectite contents derived from surface area data vary from 1 to 41% in proportion to their sand content.

## **5.2. The Hampshire Basin**

Gilkes (1966, 1968) carried out a large number of analyses from both Eocene and Oligocene strata in the Hampshire Basin. He showed that although there was much variation in detail, two main clay mineral suites were present. The first assemblage, predominantly representing non-marine facies, was composed of kaolinite and illite and he suggested that it was derived from the Cornubian granites. Gilkes (1966, 1968) suggested that the kaolinitic assemblage derived from the granites was diluted by mica-bearing sediments during its eastward passage according to the intensity of erosion prevailing. The second assemblage, associated with

marine facies, is composed of illite and smectite and is more abundant in the north and east of the basin. Trace quantities of chlorite were ascribed to a diagenetic origin. Samples from the Reading Beds from Alum Bay and Whitecliffe Bay examined by Gilkes (1968) belong to the kaolinite-illite assemblage with only traces of smectite and chlorite identified.

Blondeau and Pomerol (1968) have also described the clay mineralogy of the Tertiary strata of southern England. The clay fraction of the Woolwich Beds were found to comprise only kaolinite in the sandier horizons and kaolinite with minor illite and smectite in the clay horizons. The clay fractions of the Reading Formation were found to comprise major illite with minor kaolinite and no smectite.

Buurman (1980) also studied the clay mineralogy of the Reading Beds from Alum Bay. Mica and kaolinite were found to dominate the clay mineralogy with variable smectite content and minor quantities of chlorite. Quartz, hematite, goethite and calcite were also identified in the  $<1 \mu\text{m}$  clay fractions. Buurman (1980) disagreed with the terrestrial and marine sources suggested by Gilkes (1968) and argued that pedogenesis could account for both kaolinite- and smectite-rich assemblages.

Data from the present study confirm the illite and kaolinite-dominated with minor smectite clay mineralogy of the Reading Formation at Alum Bay. The smectite-dominated assemblage at 18.9 m above the Chalk in Alum Bay was also identified by Buurman (1980). Similar smectite-dominated clay assemblages were noted at Newhaven and Michelmarsh. The non-clay mineralogy of quartz, hematite, goethite and calcite is also similar to that identified by Buurman (1980).

### **5.3. Origin of clay minerals**

The mudstones and clay matrices of the Lambeth Group in both the London and Hampshire basins are formed of fine-grained clay mineral intergrowths. The nature of the individual clay minerals forming such intergrowths cannot be resolved by the SEM technique. XRD analyses, coupled with the composite chemistry determined on a  $1\text{-}2 \mu\text{m}^3$  scale by EDXA, indicate that the intergrowths comprise smectite, illite and kaolinite. It is likely that the intergrowths started to develop during early diagenesis from detrital assemblages.

Several models have been proposed by other workers (see Sections 5.1 and 5.2) to explain the clay assemblages observed. The presence of dominant kaolinite in the Reading Formation would suggest the Cornubian batholith as an obvious source (Gilkes, 1968). This is further supported by heavy mineral evidence suggesting the Cornubian Massif contributed much of the detrital sand input (Blondeau and Pomerol, 1968). However, heavy mineral analysis of the Thanet Sands below and Harwich Formation above suggests a more northerly, Scottish provenance for these formations (Morton, 1992). A possible modification to this scenario is the *in situ* development of kaolinite by near-surface weathering, particularly in the Reading Formation. However, the majority of the kaolinite is very fine-grained and intimately intergrown with the other clay minerals.

In addition, rare authigenic kaolinite books develop in the Reading Formation. Their presence, coupled with the clay fabrics, extensive mottling by iron oxides, calcite precipitation in nodules and as relatively coarse crystals within the clay fabric, and filled and open root channels would support the extensive pedogenesis proposed by Buurman (1980). The kaolinite books are likely to have developed by alteration of detrital micas (Psyrillos et al., 1999) during the pedogenesis. It is unlikely that these books could survive transport over large distances.

#### **5.4. Mineralogical and petrographical controls on engineering properties**

The engineering properties of the Lambeth Group are largely controlled by the distribution of clay minerals and in particular smectite. Although clay minerals occur in both sandy and clay laminae throughout the Lambeth Group, their fabrics vary significantly. In the sand laminae the clay forms grain coatings and pore-filling matrix. In clay laminae soil-forming processes have modified the fabric and altered the mineralogy. Nevertheless, in all lithologies, porewater movement can be expected. In the interlaminated clays and sands some sand lenses retain a very open, highly permeable porosity. In areas modified by pedogenesis, the presence of calcite concretions and iron oxyhydroxide precipitates along cracks and in voids demonstrates that open pathways are present. Hence changes in porewater pressures and continued (although reduced) alteration can be expected.

A key property of the glauconitic sands of the Upnor Formation, and indeed all sandy horizons throughout the Lambeth Group, is the lack of a competent cementing phase. Hence

these sands have little inherent stability, and are likely to be unstable in vertical section. Slope stability problems may be encountered in local smectite-rich clay beds. In addition they have variable, often high, porosities which in many areas are likely to have high permeability.

## 6. CONCLUSIONS

This study of the mineralogy and petrography of the Upnor, Reading and Woolwich Formations of the Lambeth Group confirms much of the findings of previous workers but provides new information about the most likely origins of the clay minerals. The mudstones and clay matrices of the Lambeth Group are formed of fine-grained clay mineral intergrowths, comprising smectite, illite and kaolinite. Development of the intergrowths was initiated during early diagenesis from detrital assemblages.

Rare kaolinite books in the Reading Formation formed *in situ* as part of the near surface weathering which resulted in the formation of extensive iron oxyhydroxide mottling, calcite precipitation and modification of the clay fabrics. The high proportion of kaolinite in the Hampshire Basin plus evidence from heavy minerals suggest the Cornubian batholith as a likely source of the detrital material.

The engineering properties of the Lambeth Group will be influenced by a combination of:

- distribution of smectite in the clay fraction
- the distribution of the clay fraction as a variable cement to sands and as clay laminae
- the nature of open porosity for porewater movement occurring in
  - poorly cemented sand lenses
  - open root channels
  - open pathways developed during soil-forming processes between peds (*sensu lato*) and along cracks and joints now lined by calcite and iron oxides such as goethite, hematite and lepidocrocite.

## 7. REFERENCES

- Avery, B.W., Stephen, I., Brown, G. and Yaalon, D.H. 1959. *Journal of Soil Science*, **10**, 177.
- Bateman R.M. and Moffat, A.J. 1987. Petrography of the Woolwich and Reading Formation (Late Palaeocene) of the Chiltern Hills, Southern England. *Tertiary Research*, **8(3)**, 75-105.
- Blondeau, A. and Pomerol, C.H. 1968. A contribution to the sedimentological study of the Palaeogene of England. *Proceedings Geologists Association*, **79**, 441-445.
- Buurman, P. 1980. Palaeosols in the Reading Beds (Paleocene) of Alum Bay, Isle of Wight, U.K. *Sedimentology*, **27**, 593-606.
- Ellison, R.A., Knox, R.W.OB., Jolley, D.W. and King, C. 1994. A revision of the lithostratigraphical classification of the early Palaeogene strata of the London Basin and East Anglia. *Proceeding of the Geologists Association*, **105**, 187-197.
- Ellison, R.A., Ali, J.A., Hine, N.M. and Jolley, D.W. 1996. Recognition of Chron C25n in the upper Paleocene Upnor Formation of the London Basin, UK. In: Knox, R.W.OB., Corfield, R.M. and Dunay, R.E. (Eds.) 1996. *Correlation of the Early Paleogene in Northwest Europe, Geological Society Special Publication*, **101**, 185-193.
- Gilkes, R.J. 1966. The clay mineralogy of the Tertiary sediments of the Hampshire Basin. *Ph.D. thesis*. University of Southampton.
- Gilkes, R.J. 1968. Clay mineral provinces in the Tertiary sediments of the Hampshire Basin. *Clay Minerals*, **7**, 351-362.
- Kemp, S.J. and Pearce, J.M. 1992. A mineralogical and geochemical study of pyrite alteration: Implications for trace element mobility and radionuclide migration. *Nirex Safety Studies Research Report NSS/R317*.
- Knox, R.W.OB. 1996. Tectonic controls on sequence development in the Palaeocene and earliest Eocene of southeast England: implications for North Sea stratigraphy. In: Hesselbo, S.P. and Parkinson, D.N. (Eds.) *Sequence Stratigraphy in British Geology, Geological Society Special Publication*, **103**, 209-230.
- Knox, R.W. OB. 1997. Personal Communication.
- Morton, A.C. 1982. The provenance and diagenesis of Palaeocene sandstones of southeast England, as indicated by heavy minerals analysis. *Proceedings of the Geologists Association*, **93**, 263-274.
- Perrin, R. M. S. 1971 The clay mineralogy of British sediments. *Mineralogical Society (Clay Minerals Group)*, London.

Psyrillos, A., Howe, J.H., Manning, D.A.C. and Burley, S.D. 1999. Geological controls on kaolin particle shape and consequences for mineral processing. *Clay Minerals*, **34**(1), 193-202.

Rae, J.E. and Parker, A. 1992. Groundwater quality in the recharged London Basin, England I: Phase associations of iron, manganese, and sulphur in Tertiary sands. *Environmental Geology Water Science*, **19**, 127-135.

Weir, A.H. and Catt, J.A. 1969. The mineralogy of some Palaeogene samples from Kent. *Sedimentary Geology*, **3**, 17-33.

Table 1. Sample localities and descriptions (London Basin)

Location	Sample	Metres above Chalk	MPG code	Fm.	Description
Newbury	NB18	1.15	H488	Upnor	Medium grey stiff clay
	NB19	1.35	H489	Upnor	Medium grey stiff clay
	NB3	1.50	H473	Upnor	Medium grey, soft clay admixed with buff medium-grained sand
	NB4	2.00	H474	Upnor	Pale grey/buff medium-grained sand with plastic clay
	NB1	2.25	H471	Reading	Medium grey/buff firm clay
	NB2	2.75	H472	Reading	Pale grey, firm clay
	NB5	3.50	H475	Reading	Pale buff fine-grained sand with clay
	NB6	4.75	H476	Reading	Pale grey, laminated siltstone, with some darker laminae
	NBS3	5.00	H494	Reading	Pale grey soft clay with red spots
	NB7	5.35	H477	Reading	Pale cream, friable siltstone
	NB8	5.80	H478	Reading	Plastic medium-grey clay with patches of heavy rusty staining
	NB9	6.20	H479	Reading	Fine-grained buff-coloured sand, with some Fe-staining
	NB10	7.80	H480	Reading	Pale-grey, fine-grained sand
	NB11	8.50	H481	Reading	Medium grey/green siltstone with ?goethite blebs
	NBS2	8.50	H509	Reading	Pale grey, firm clay with some Fe-stained horizons
	NB12	10.00	H482	Reading	Pale grey fine silt/claystone with some Fe staining
	NB20	11.00	H490	Reading	Rusty-coloured medium-grained loose sand
	NBS1	11.20	H493	Reading	Pale grey with reddened streaks, stiff clay
	NB13	12.10	H483	Reading	Pale grey firm clay with patches of Fe-staining
	NB14	12.70	H484	Reading	Dark grey laminated clay
	NB15	13.30	H485	Reading	Medium grey/buff clay
	NB27C	13.60	H508	Reading	Pale grey, hard clay with red streaks/patches
	NB27A	14.70	H507	Reading	Rusty coloured firm clay
NB26	18.90	H492	Reading	Medium buff, medium-grained sand	
NB17	19.05	H487	Reading	Rusty coloured clay admixed with some fine-grained sand	
NB16	19.70	H486	Reading	Medium brown, Fe-stained plastic sandy clay	
NB25A	20.00	H505	Reading	Medium grey soft clay, with some Fe-staining and sandy patches	
NB25B	20.25	H506	Reading	Pale grey/buff clay	
NB24	-	H504	Reading	Pale-medium grey (rusty), soft clay, with medium-grained sand	
NB23	-	H491	Reading	Medium red/grey clay	
Copyhold Fm	-	-	D835	Reading	Pale buff medium-grained unconsolidated sand
M40	M40/2	-	H503	Reading	Medium brown siltstone
Hermitage Fm	HF1	-	D836	Reading	Pale buff fine-grained unconsolidated sand
Chievely Pit	C1	-	D838	Reading	Pale buff medium unconsolidated sand
	C2	-	D839	Reading	Pale grey/buff plastic clay with some rusty staining
Orsett Quarry	OQ1	2.80	H495	Upnor	Pale grey clay admixed with medium-grained ?goethite-coated sand
	OQ2	4.00	H496	Upnor	Medium grey, weakly laminated, friable siltstone
	OQ3	5.00	H497	Upnor	Pale grey, slightly sandy, soft clay
Upnor Quarry	UQ1	4.9	H498	Upnor	Pale grey, medium-grained loose sand
	UQ2	6.3	H499	Upnor	Pale-medium grey (Fe-stained), laminated soft clay
	UQ3	7.3	H500	Upnor	Pale/medium grey fine-grained clayey sand
	UQ4	11.5	H501	Woolwich	Dark grey siltstone with abundant white shell fragments (?bivalves)
	UQ5	12.34	H502	Woolwich	Green/brown clay with abundant white shell fragments
Glazenwood	G1	-	D845	Reading	Medium brown, plastic clay
	G2	-	D846	Reading	Medium brown, plastic clay
	G3	-	D847	Reading	Dark brown plastic clay
Enfield	E1	-	D848	?	Pale grey, laminated sandy clay with pervasive rusty staining
	E2	-	D849	Reading	Dry, hard medium buff silty clay with some surficial red staining
	E3	-	D850	Reading	Dry, hard medium buff silty clay with some surficial red staining
	E4	-	D851	Reading	Medium grey, friable silty clay
	E5	-	D852	Reading	Dry, hard pale grey/buff clay, with some rusty staining



**Table 2. Sample localities and descriptions (Jubilee Line Extension BH 404T)**

Depth (mbgl)	Lithostatigraphy	Description
24.11	Upper Shelly Clay	Olive grey, bioturbated, silty clay with <i>Corbicula</i> and <i>Typanotonus</i> ?
24.79	Upper Shelly Clay	Olive grey silty sand with disarticulated shells.
25.35	Upper Mottled Clay	Olive grey or pale brown sandy silt or silty sand.
26.00	Upper Mottled Clay	Heavily fissured, mottled blue grey and pale brown silty clay
26.38	Upper Mottled Clay	Heavily fissured, mottled mainly pale red brown with blue grey, silty clay.
27.95	Upper Mottled Clay	Heavily fissured, mottled blue grey and pale brown silty clay + red patches.
28.68	Upper Mottled Clay	Heavily fissured, mottled mainly pale red brown with blue grey, silty clay.
28.87	Upper Mottled Clay	Heavily fissured, mottled mainly blue grey, with pale brown, silty clay.
29.87	Upper Mottled Clay	Bioturbated, medium grey, silty clay.
30.11	Laminated sands and silts	Grey brown clayey silt/sand.
33.19	Lower Shelly Clay	Dark grey, organic clay with bivalves.
34.00	Lower Mottled Clay	Highly fractured, multicoloured, mainly white with pale purple. Calcareous?
34.18	Lower Mottled Clay	Yellow brown, dark grey and pale green grey mottled silty clay.
34.87	Lower Mottled Clay	As above but mottling blue grey, dark red/purple and yellow brown.
35.04	Lower Mottled Clay	Greenish grey and yellow brown silty clay. From chalk and flint lens.
35.12	Lower Mottled Clay	Pale yellow brown, greenish grey and purple mottled, silty clay.

**Table 3. Sample localities and descriptions (Hampshire Basin)**

Sample site	Depth (m)	MPG code	Description
Alum Bay	0.3	D813	Medium brown, friable, clayey sand
	2.9	D814	Rusty-brown/grey, firm, slightly friable clay
	4.7	D815	Medium grey, friable clay with abundant rusty coloured spots
	6.0	D816	Medium brown/grey, friable clay with abundant rusty coloured spots
	7.6	D817	Dark grey, friable clay with abundant rusty spots
	11.3	D818	Firm, medium brown/grey clay
	13.6	D819	Medium grey/brown, firm, slightly friable clay, with rusty staining
	15.3	D820	Grey/buff clayey sand
	17.0	D821	Pale grey silty clay with red (Fe-rich) spots/patches and staining
	18.9	D822	Pale grey, plastic clay with abundant dark red Fe-rich spots
	21.7	D823	Heterogeneous, red and pale grey clay, Fe staining
	22.6	D824	Medium rusty brown coloured, dry, friable, stony clay with red spots
	23.0	D825	Medium brown/grey, firm clay with rusty-coloured spots
	24.2	D826	Medium red/brown, firm clay
	26.1	D827	Medium-grey and red, soft silty clay
	27.5	D828	Medium red/brown, firm clay
	28.5	D829	Pale-medium grey firm clay with red, Fe-rich spots
30.0	D830	Medium grey, firm clay with abundant red, Fe-rich patches	
31.1	D831	Firm, dark grey clay with red, Fe-rich spots	
35.2	D832	Pale grey, friable clay with abundant red, Fe-rich patches and staining	
38.3	D833	Medium grey, firm clay with red, Fe-rich spots and staining	
40.5	D834	Medium grey, firm clay with red, Fe-rich patches	
Newhaven	-	D837	Rusty orange/brown medium-grained unconsolidated sand
Newhaven 1	-	D844	Dark brown, plastic silty clay containing some roots
Knoll Manor 1	~13.5	D840	Medium grey/buff clay with red, Fe-rich spots
Knoll Manor 2	~7.0	D841	Medium red/brown, friable silty clay
Michelmarsh	~8.0	D842	Pale grey, plastic clay with abundant red, Fe-rich patches
Whitecliffe Bay	39.5	D843	Medium grey soft clay with sparse red, Fe-rich spots

Table 4. Summary of whole-rock XRD and surface area analyses (London Basin)

Sample	Major	Minor	Trace	Surface area (m <sup>2</sup> /g)	Equivalent %smectite
NB18	Quartz, smectite	Kaolinite, mica, K-feldspar	Albite	325	41
NB19	Quartz, smectite	Mica, kaolinite, K-feldspar	Albite	240	30
NB3	Quartz	Mica	Kaolinite, K-feldspar	158	20
NB4	Quartz	Smectite, mica, K-feldspar, albite	Kaolinite	Nd	Nd
NB1	Quartz	Smectite, kaolinite, mica, K-feldspar	Albite	199	25
NB2	Quartz	Smectite, mica, K-feldspar, albite	Kaolinite	180	22
NB5	Quartz	K-feldspar	Mica	Nd	Nd
NB6	Quartz	Smectite, mica, K-feldspar	Kaolinite, albite	190	24
NBS3	Quartz	Smectite, mica, kaolinite, K-feldspar, albite	Hematite	159	20
NB7	Quartz	Mica, kaolinite, albite, K-feldspar	Smectite	134	17
NB8	Quartz	Mica, lepidocrocite, K-feldspar	Albite, kaolinite	89	11
NB9	Quartz	K-feldspar	Mica, albite	Nd	Nd
NB10	Quartz	K-feldspar	-	Nd	Nd
NB11	Quartz, smectite	Mica, kaolinite	K-feldspar, albite, ?hematite	261	33
NBS2	Quartz	Smectite, K-feldspar, mica, kaolinite	Albite, hematite	203	25
NB12	Quartz, smectite	Kaolinite, mica	K-feldspar, albite, goethite, hematite	223	28
NB20	Quartz	K-feldspar	Smectite, mica, hematite	Nd	Nd
NBS1	Quartz	Smectite, kaolinite	K-feldspar, hematite, ?goethite	155	19
NB13	Quartz	Smectite, kaolinite, mica	K-feldspar, goethite	170	21
NB14	Quartz	Mica, smectite, kaolinite	K-feldspar, albite, goethite, hematite	164	20
NB15	Quartz	Mica, smectite, kaolinite, K-feldspar	Albite, goethite, hematite	125	16
NB27C	Quartz	Smectite, kaolinite, hematite	K-feldspar, mica, goethite	188	23
NB27A	Quartz	Mica, smectite, kaolinite, K-feldspar	Albite, hematite, ?goethite	129	16
NB26	Quartz	K-feldspar	Mica, hematite	Nd	Nd
NB17	Quartz	K-feldspar, mica, kaolinite	Albite	57	7
NB16	Quartz	Mica, kaolinite	K-feldspar, albite	83	10
NB25A	Quartz	Mica, K-feldspar, smectite, kaolinite	Albite	184	23
NB25B	Quartz	K-feldspar, mica, smectite, kaolinite	Albite, hematite	85	11
NB24	Quartz	K-feldspar, mica, kaolinite, smectite	?Goethite	185	23
NB23	Quartz	Smectite, mica, K-feldspar, kaolinite, albite	Hematite	135	17

Table 4. (continued) Summary of whole-rock XRD and surface area analyses (London Basin)

Sample	Major	Minor	Trace	Surface area (m <sup>2</sup> /g)	Equivalent %smectite
Copyhold Farm	Quartz	K-feldspar	?Jarosite	6	1
M40/2	Quartz	Mica, kaolinite, K-feldspar, smectite	Albite, ?goethite	132	17
HF1	Quartz	K-feldspar	Albite, mica	27	3
C1	Quartz	-	K-feldspar, ?jarosite	187	23
C2	Quartz, smectite	Mica, kaolinite	K-feldspar, albite	4	1
OQ1	Quartz, smectite	Mica, kaolinite	K-feldspar	276	34
OQ2	Quartz	Smectite, mica, kaolinite	K-feldspar, ?goethite	128	16
OQ3	Quartz	Smectite, kaolinite, mica	Albite, hematite	115	14
UQ1	Quartz	K-feldspar	Albite	Nd	Nd
UQ2	Quartz	Smectite, mica, K-feldspar, kaolinite	Albite	151	19
UQ3	Quartz	Kaolinite	-	21	3
UQ4	Quartz	Gypsum, smectite, aragonite	Kaolinite, mica, ?pyrite	181	23
UQ5	Quartz	Aragonite, smectite, mica	?Pyrite, ?goethite	126	16
G1	Quartz	Calcite, kaolinite, mica	Albite, K-feldspar, ?smectite	51	6
G2	Quartz	Kaolinite, mica, calcite	Albite, K-feldspar, goethite	176	22
G3	Quartz	Kaolinite, mica, calcite	K-feldspar, albite, ?goethite, ?smectite	176	22
E1	Quartz, smectite	Kaolinite	Mica, albite, K-feldspar	239	30
E2	Quartz	-	Kaolinite, mica, albite, K-feldspar	175	22
E3	Quartz	Kaolinite, mica	Albite, K-feldspar	163	20
E4	Quartz	Kaolinite, mica	Albite, K-feldspar	155	19
E5	Quartz, smectite	Kaolinite, mica	Goethite, K-feldspar	216	27

Nd – not determined

Table 5. Summary of whole-rock XRD and surface area analyses (Hampshire Basin)

Sample site	Metres above Chalk	Major	Minor	Trace	Surface area (m <sup>2</sup> /g)	Equivalent %smectite
Alum Bay	0.3	Quartz	-	Calcite, mica, ?feldspar	64	8
	2.9	Quartz	Kaolinite, mica, goethite	Albite, K-feldspar	129	16
	4.7	Quartz	Kaolinite, mica, goethite	Albite, K-feldspar	92	12
	6.0	Quartz	Kaolinite, mica, goethite	Albite, K-feldspar	108	13
	7.6	Quartz	Mica, kaolinite	K-feldspar, ?albite	163	20
	11.3	Quartz	Kaolinite, mica, goethite	Albite, K-feldspar	125	16
	13.6	Quartz	Kaolinite, mica, goethite	Albite, K-feldspar, smectite	111	14
	15.3	Quartz	-	Kaolinite, mica, ?K-feldspar	38	5
	17.0	Quartz	Kaolinite, mica	K-feldspar, albite	62	8
	18.9	Quartz, smectite	Kaolinite, mica	K-feldspar, albite, hematite	148	18
	21.7	Quartz	Kaolinite, hematite, goethite	Smectite, K-feldspar	117	15
	22.6	Quartz	Goethite, kaolinite	Hematite, ?K-feldspar	70	9
	23.0	Quartz	Kaolinite	K-feldspar	113	14
	24.2	Quartz	Kaolinite, mica, goethite	K-feldspar, albite	154	19
	26.1	Quartz	-	Mica, kaolinite, ?K-feldspar, ?hematite	55	7
	27.5	Quartz	Kaolinite, mica	Albite, K-feldspar, ?goethite	130	16
	28.5	Quartz	Kaolinite, mica	K-feldspar, albite	104	13
	30.0	Quartz	Kaolinite, hematite, goethite	Mica, albite, K-feldspar	118	15
	31.1	Quartz	Mica, kaolinite, goethite	Albite, K-feldspar	159	20
	35.2	Quartz	Mica, kaolinite	Albite, K-feldspar, ?hematite	88	11
38.3	Quartz	Kaolinite, mica	K-feldspar, albite	100	13	
40.5	Quartz	Mica, kaolinite, smectite	K-feldspar, albite, ?hematite	89	11	
Newhaven	-	Quartz	Jarosite	K-feldspar, ?Albite, ?pyrite	26	3
Newhaven 1	-	Quartz	Smectite, kaolinite, mica, halite, pyrite	K-feldspar, ?albite	171	21
Knoll Manor 1	~13.5	Quartz	Kaolinite, mica, halite	K-feldspar, albite, hematite	138	17
Knoll Manor 2	~7.0	Quartz	Mica, kaolinite	Goethite, albite, K-feldspar, hematite	69	9
Michelmarsh	~8.0	Quartz	Mica, kaolinite, smectite	Hematite, K-feldspar, albite, ?goethite	167	21
Whitecliffe Bay	39.5	Quartz	Mica, kaolinite	Smectite, K-feldspar, albite, ?hematite	172	22

**Table 6. Summary of surface area analyses (Jubilee Line Extension BH 404T)**

<b>Sample Depth mbgl</b>	<b>Surface area (m<sup>2</sup>/g)</b>	<b>Equivalent %smectite</b>
24.11	42	5
24.79	115	14
25.35	12	2
26.00	136	17
26.38	195	24
27.95	210	26
28.68	172	22
28.87	229	29
29.87	252	32
30.11	126	16
33.19	234	29
34.00	147	18
34.18	387	48
34.87	319	40
35.04	264	33
35.12	269	34

**Table 7. Summary of <2 µm XRD analyses (London Basin)**

Sample	Major	Minor	Trace
NB18	Smectite	Illite, kaolinite	-
NB19	Smectite	-	Illite, kaolinite
NB3	Smectite	Illite, kaolinite	-
NB4	Smectite	Illite, kaolinite	-
NB1	Smectite	Kaolinite, illite	-
NB2	Smectite	Kaolinite, illite	-
NB5	Smectite	Illite, kaolinite	-
NB6	Smectite	Kaolinite, illite	-
NBS3	Smectite	Illite, kaolinite	-
NB7	Kaolinite	Illite, goethite	Smectite, lepidocrocite
NB8	Smectite	Illite, kaolinite, lepidocrocite	-
NB9	Illite	Kaolinite, lepidocrocite	Smectite, goethite
NB10	Smectite	Kaolinite, illite	-
NB11	Smectite	Kaolinite, illite	Goethite
NBS2	Smectite	Kaolinite	Illite, goethite
NB12	Smectite	Kaolinite	Illite, goethite
NB20	Illite	Kaolinite	Smectite
NBS1	Kaolinite	Smectite, goethite	Illite
NB13	Smectite	Kaolinite	Illite, goethite
NB14	Illite	Kaolinite, smectite	Goethite
NB15	Kaolinite	Smectite, illite	Goethite
NB27C	Smectite	Illite, kaolinite	Lepidocrocite, goethite
NB27A	Smectite	Illite, kaolinite	Goethite
NB26	Kaolinite	Illite, smectite	-
NB17	Smectite	Kaolinite, illite	Goethite
NB16	Illite, kaolinite	Smectite	Goethite
NB25A	Smectite	Kaolinite, illite	Goethite
NB25B	Smectite	Illite, kaolinite	-
NB24	Kaolinite	Smectite, illite, goethite	Goethite
NB23	Smectite	Illite, kaolinite	-
Copyhold Farm	Smectite	Kaolinite, illite	-
M40/2	Smectite	Kaolinite, illite	Goethite
Hermitage Farm	Smectite	Kaolinite, illite	-
Chievely Pit	Smectite	Kaolinite, illite	-
Chievely Pit	Smectite	Kaolinite, illite	Goethite
OQ1	Smectite	Illite, kaolinite	-
OQ2	Smectite	Kaolinite, illite	-
OQ3	Smectite, kaolinite	Illite	-
UQ1	Smectite	Kaolinite, illite	-
UQ2	Smectite	Kaolinite, illite	-
UQ3	Kaolinite	-	Smectite, illite
UQ4	Smectite	Lepidocrocite	Illite, kaolinite, goethite
UQ5	Smectite	Illite, kaolinite	Goethite
G1	Smectite	Kaolinite, illite	Goethite
G2	Smectite	Kaolinite, illite	Goethite
G3	Smectite	Kaolinite, illite	Goethite, chlorite
E1	Smectite	Kaolinite, illite	Goethite, ?chlorite
E2	Smectite	Kaolinite, illite	Goethite
E3	Smectite	Kaolinite, illite, chlorite	-
E4	Smectite	Kaolinite, illite	Chlorite
E5	Smectite	Kaolinite, illite	Goethite

Table 8. Summary of <2 µm XRD analyses (Hampshire Basin)

Sample site	Metres above Chalk	Major	Minor	Trace
Alum Bay	0.3	Illite	Kaolinite, smectite	-
	2.9	Kaolinite	Illite, smectite	Goethite
	4.7	Kaolinite	Illite, smectite	Goethite
	6.0	Kaolinite	Illite, smectite	Goethite
	7.6	Illite	Kaolinite	Goethite
	11.3	Kaolinite	Illite	Chlorite, smectite, goethite
	13.6	Kaolinite	Illite, smectite	Goethite, chlorite
	15.3	Kaolinite	Illite, smectite	-
	17.0	Kaolinite	Smectite, illite	-
	18.9	Smectite	Kaolinite, illite	?Goethite
	21.7	Kaolinite	Smectite	Illite, goethite
	22.6	Kaolinite	Illite, smectite	Goethite
	23.0	Kaolinite	Smectite, illite	Goethite
	24.2	Kaolinite	Smectite, illite	Goethite
	26.1	Kaolinite	Smectite, illite	Goethite
	27.5	Kaolinite	Smectite, illite	-
	28.5	Kaolinite	Smectite, illite	-
	30.0	Kaolinite	Illite	Smectite, goethite
	31.1	Kaolinite	Illite, smectite	?Goethite
	35.2	Kaolinite	Illite, smectite	-
38.3	Kaolinite	Smectite, illite	-	
40.5	Kaolinite	Illite, smectite	-	
Newhaven	-	Illite	Smectite, goethite	Kaolinite
Newhaven 1	-	Smectite	Kaolinite, illite	?Goethite
Knoll Manor 1	-	Kaolinite	Illite, smectite	?Goethite
Knoll Manor 2	-	Kaolinite	Illite	Smectite, goethite
Michelmarsh	-	Smectite	Illite, kaolinite	-
Whitecliffe Bay	-	Kaolinite	Smectite, illite	-

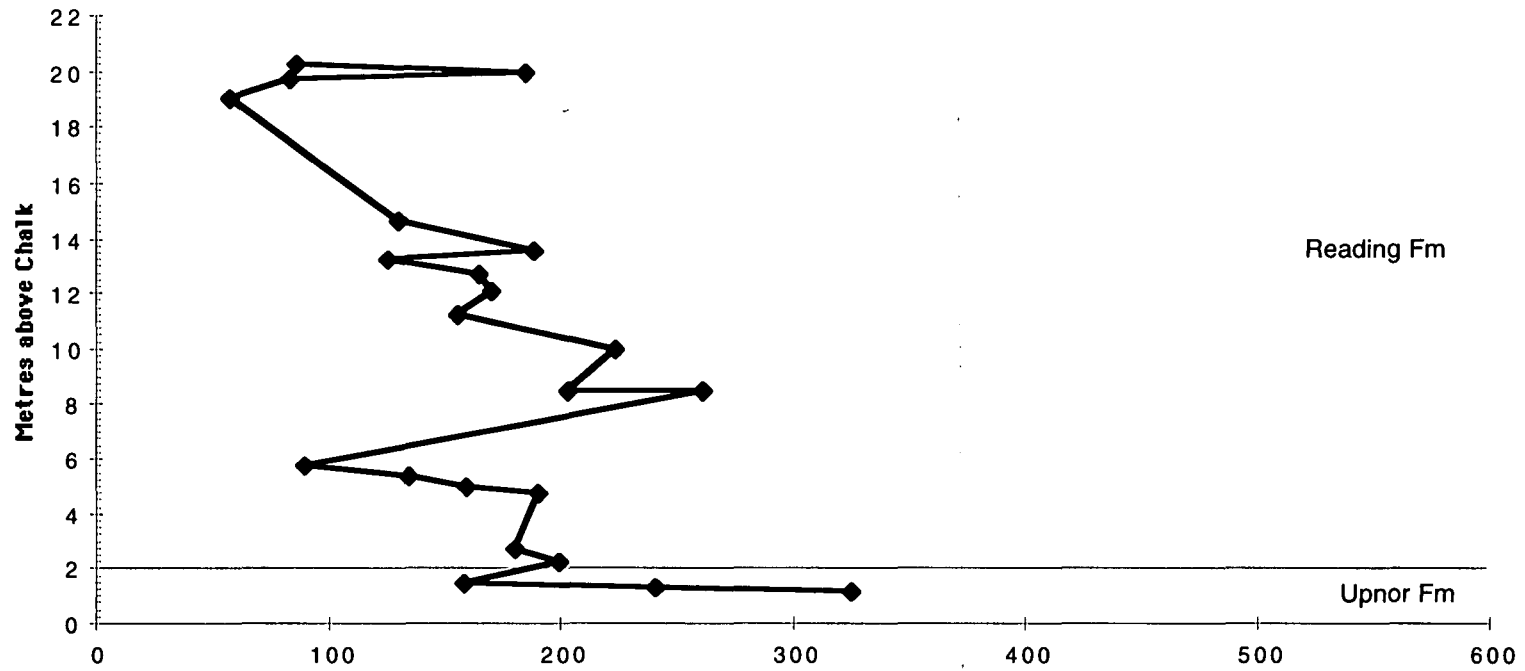


Figure 1. Stratigraphic variation of surface area for the Newbury samples



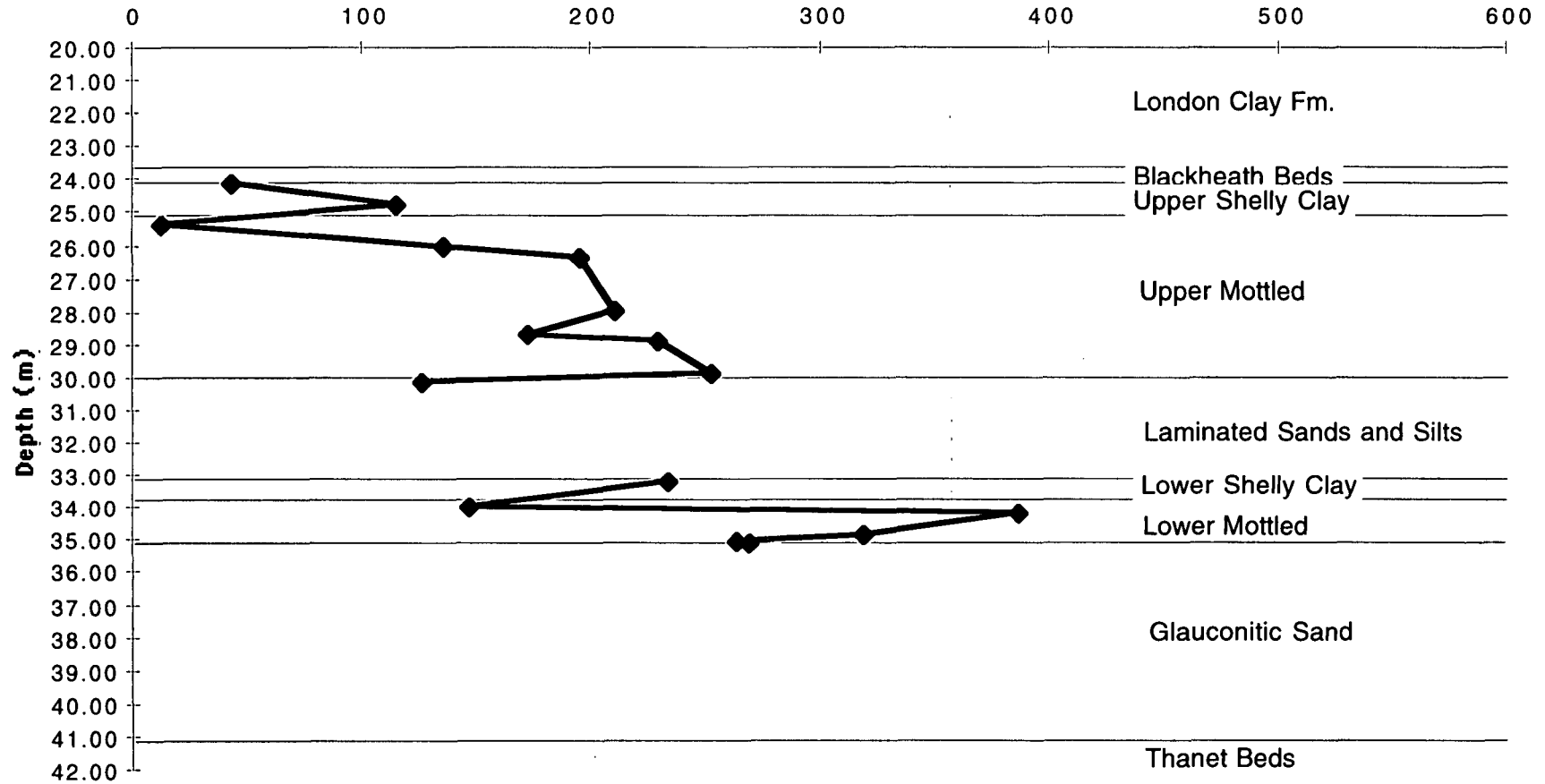


Figure 2. Downhole variation of surface area for the Jubilee Line Extension BH 404T

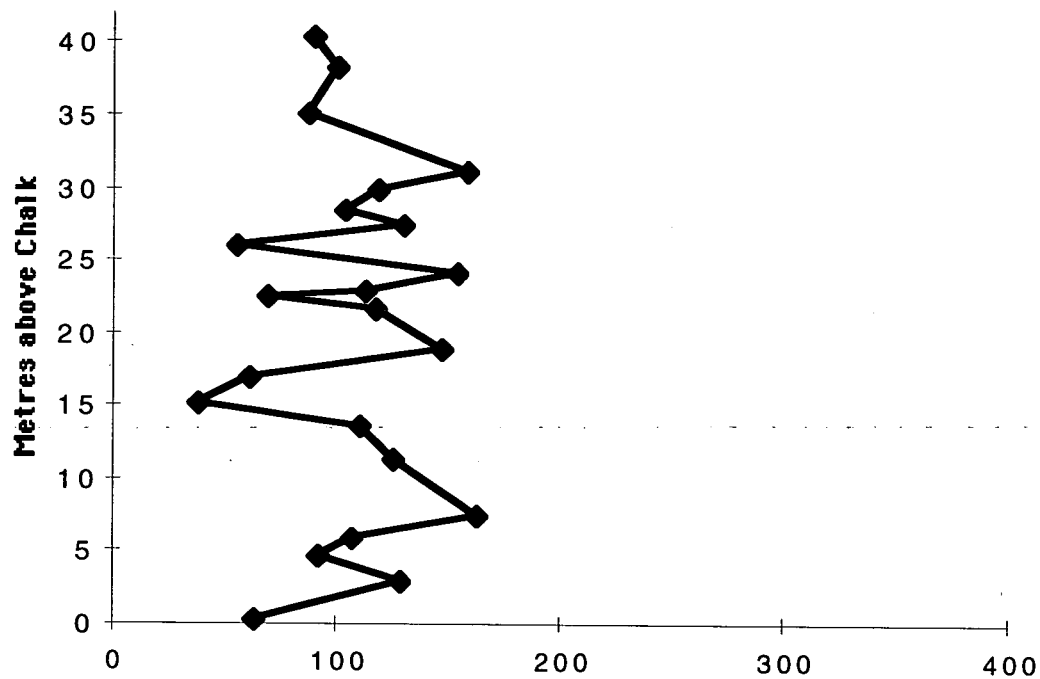


Figure 3. Stratigraphic variation of surface area for the Alum Bay



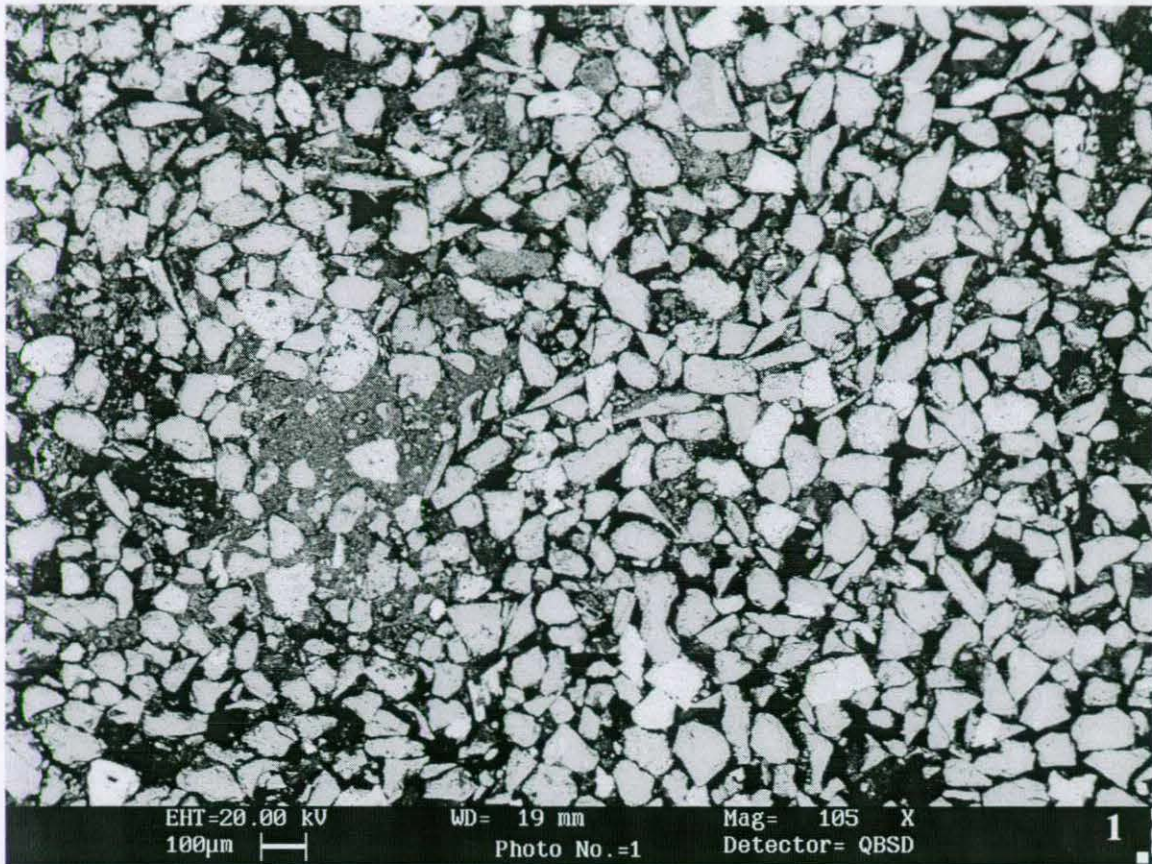


Plate 1: Typical example of Thanet Sand Formation, comprising well sorted fine grained sand, locally weakly cemented by detrital clay. Note oversized secondary voids due to feldspar dissolution. Sample JLE 52.80 m, Jubilee Line Extension BH 404T. (D789P1/01)

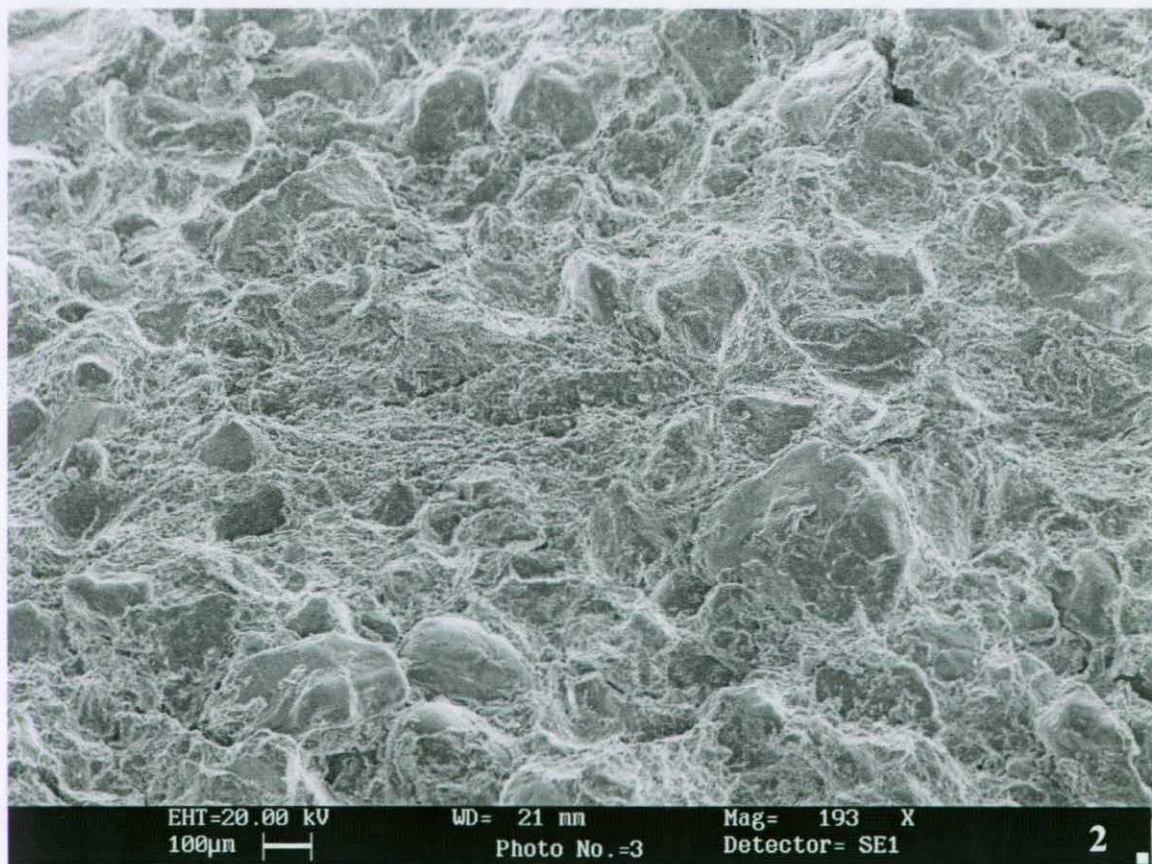


Plate 2: Typical view of moderately sorted, glauconitic sandy clay of the Upnor Formation in London Basin. Sample NB3, Newbury Bypass, 1.55-1.8m above Chalk (E439S1/03).



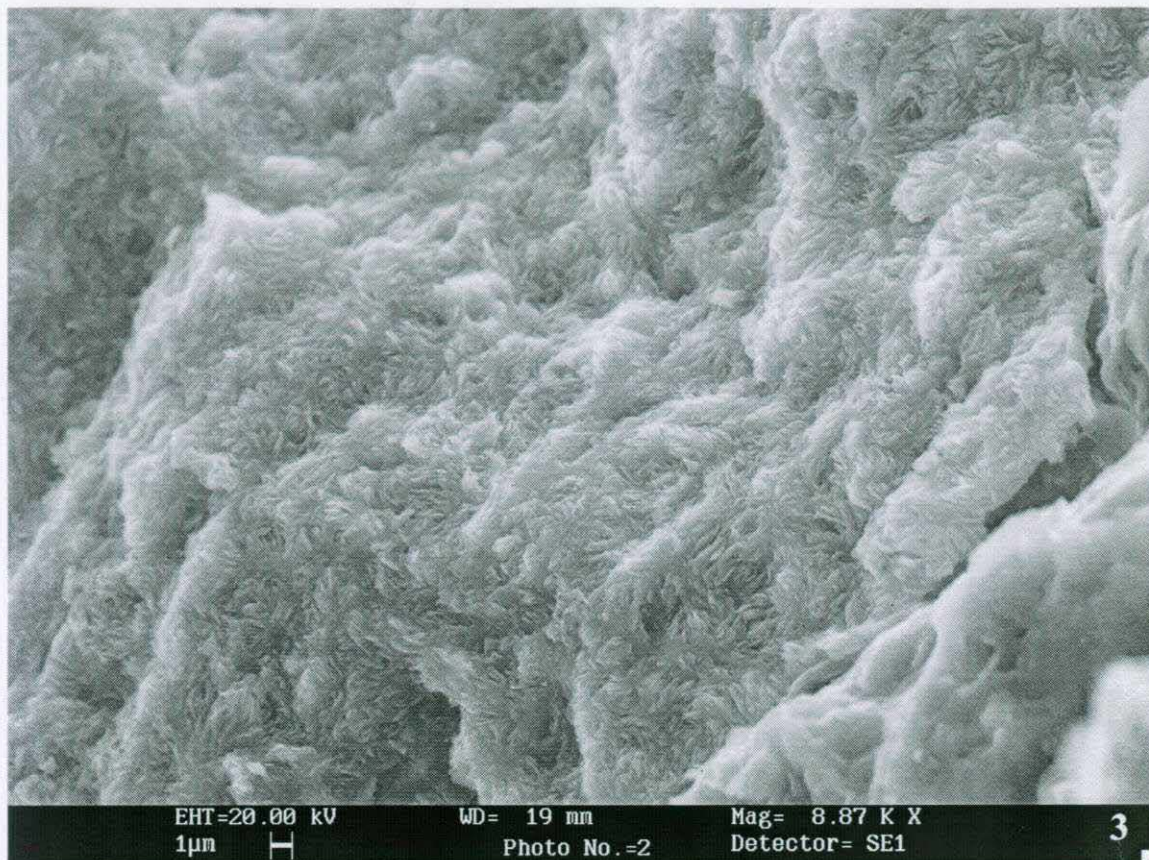


Plate 3: Internal fine-grained texture of a glauconitic sand grain in the Upnor Formation, London Basin. Sample NB3, Newbury Bypass, 1.55-1.8m above Chalk (E439S1/02).

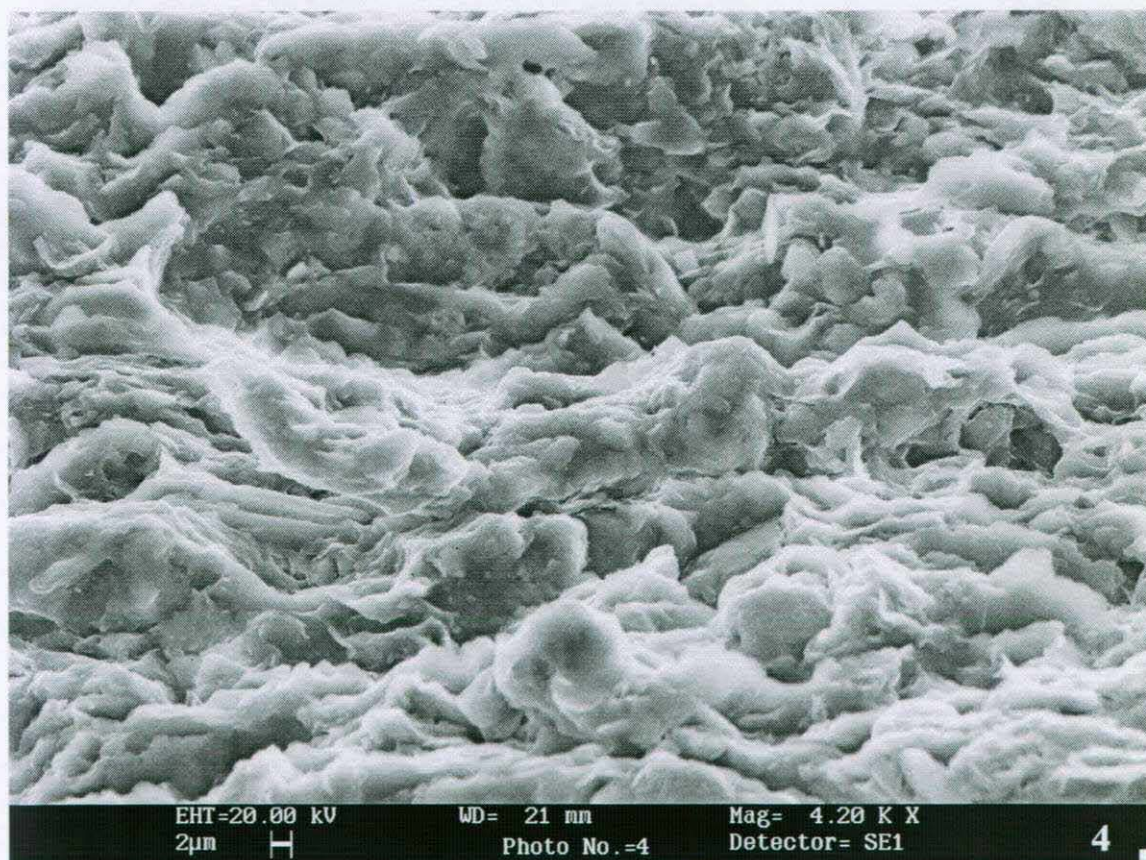


Plate 4: Compacted detrital clay matrix with no lamination from the Upnor Formation in the London Basin. Sample NB3, Newbury Bypass, 1.55-1.8m above Chalk (E439S1/04).



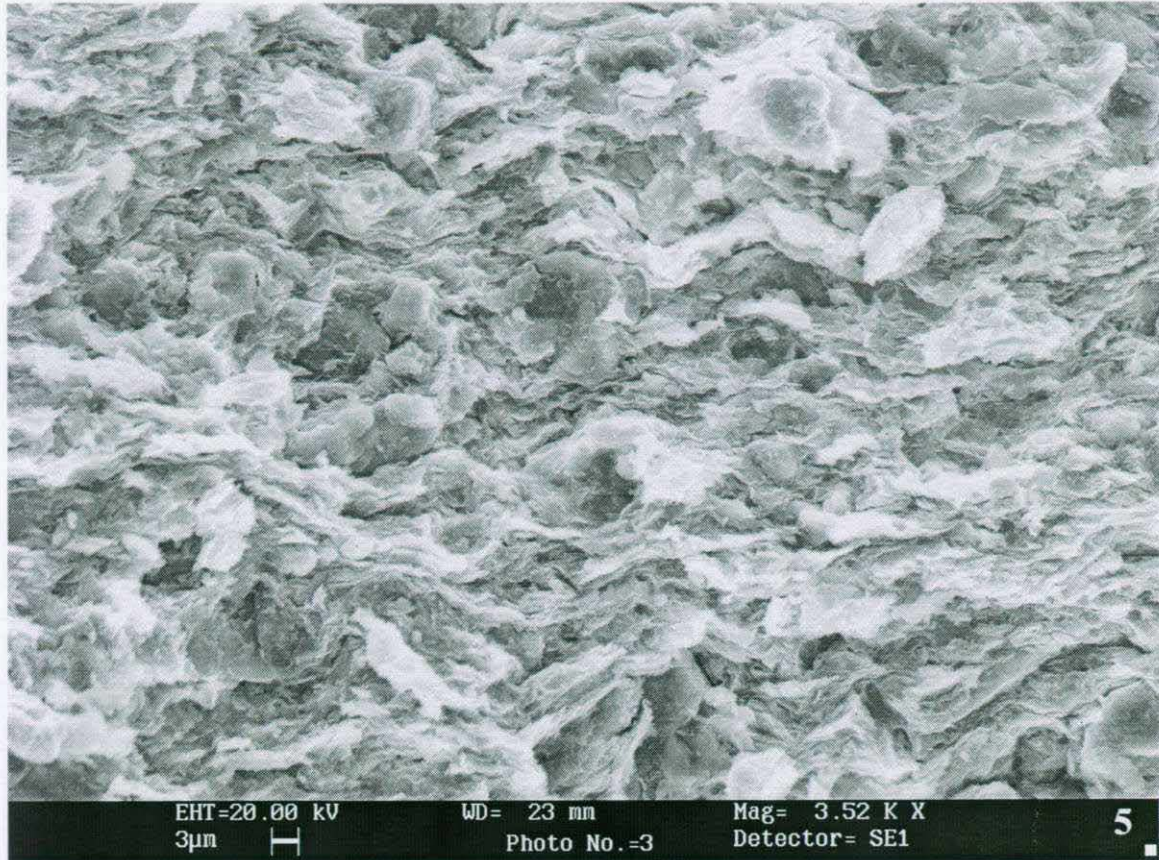


Plate 5: Compacted detrital clay matrix with a weakly developed laminated fabric in the Upnor Formation, London Basin. Sample NB3, Newbury Bypass, site G, 1.55-1.8m above Chalk (E431S1/03).

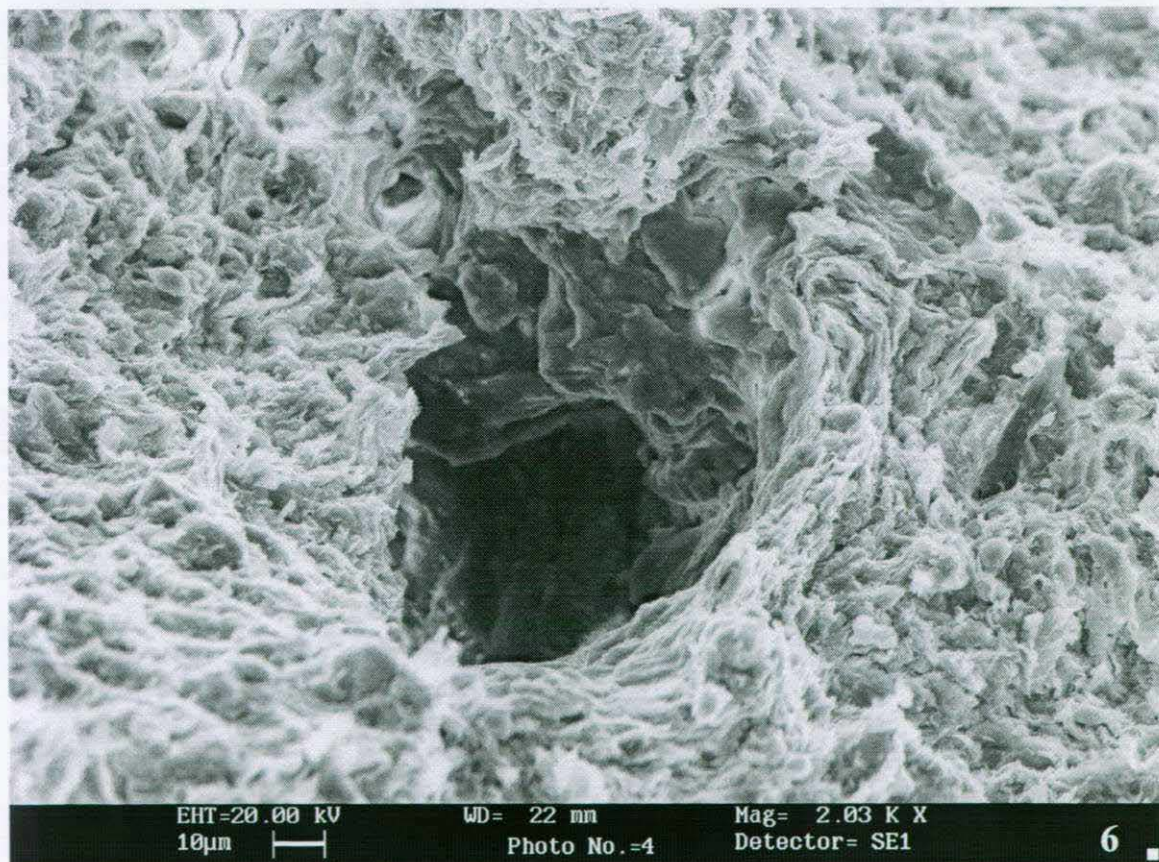


Plate 6: Open root channel with clay particles oriented around channel wall. Sample NB3, Newbury Bypass, site G, 1.55-1.8m above Chalk (E431S1/04).



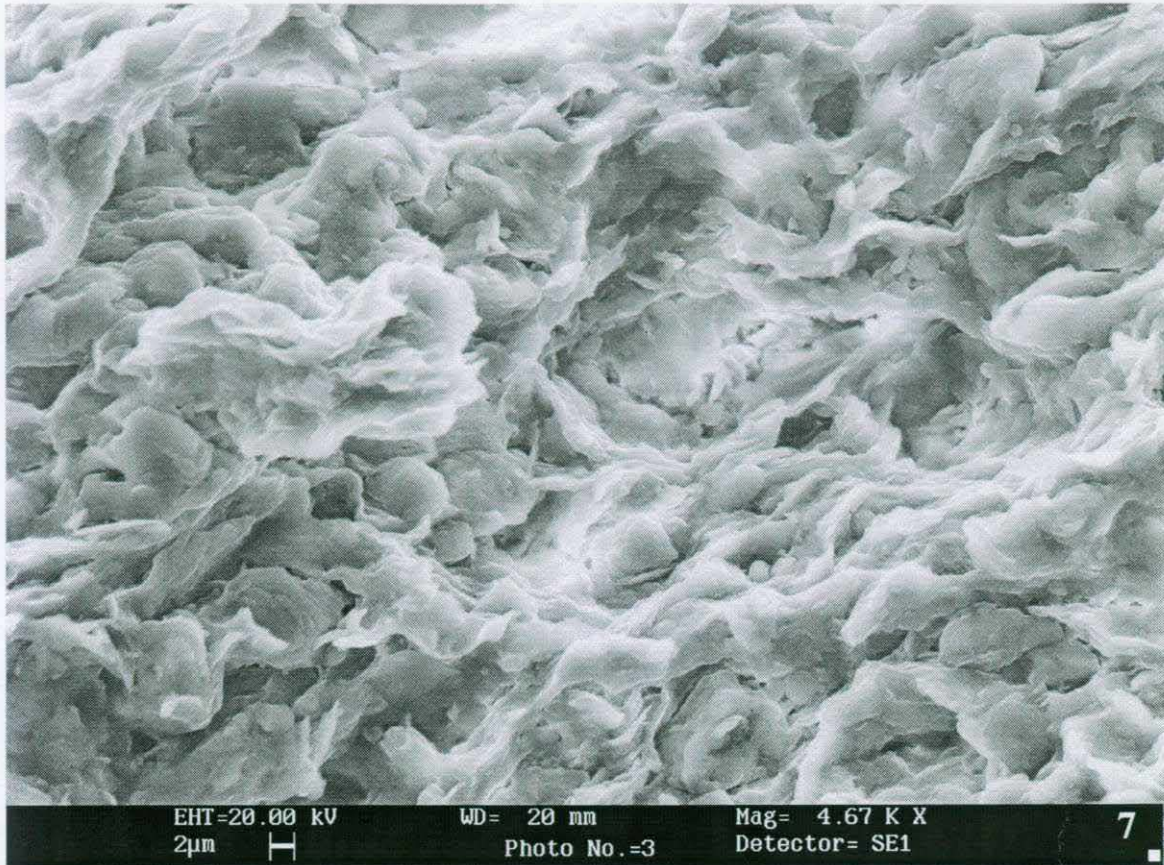


Plate 7: Detailed view of very weakly developed alignment of clay particles in the Upnor Formation, London Basin. Orsett Quarry, OQ2 (E435S1/03).

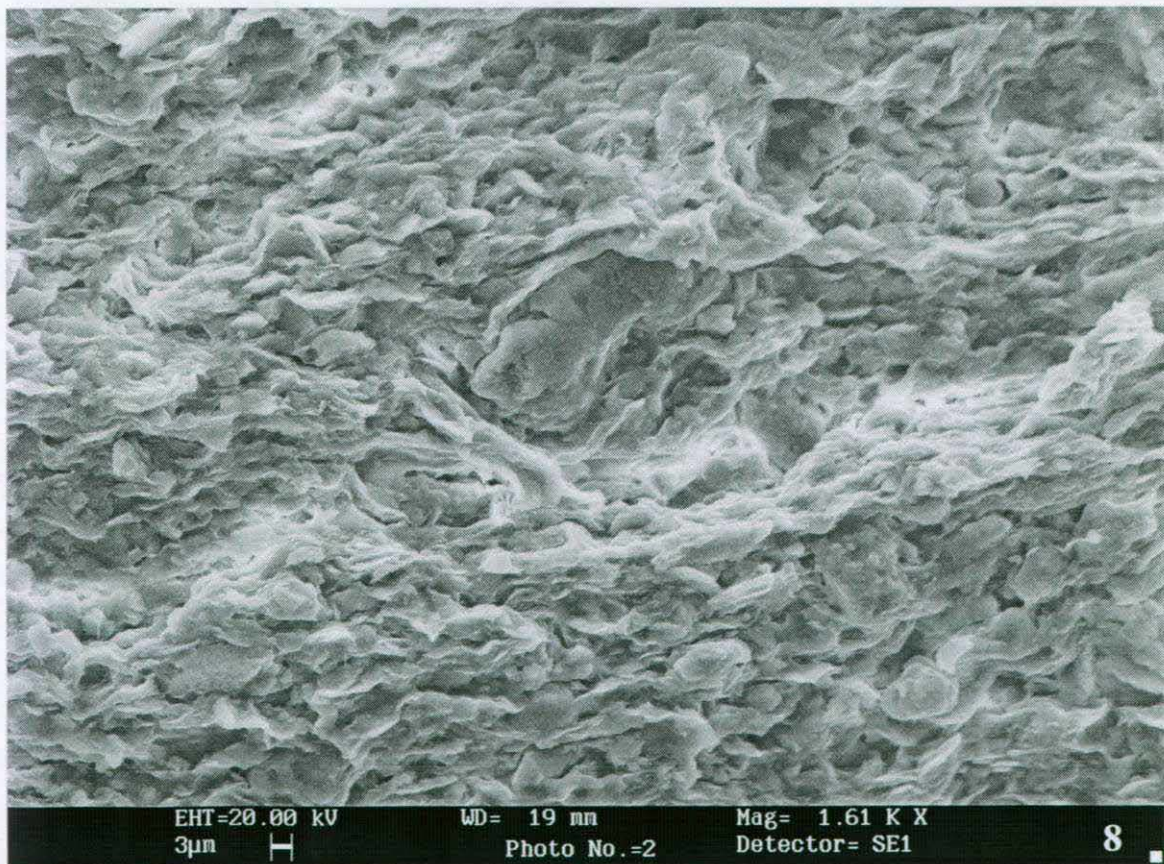


Plate 8: Detailed view of moderately developed alignment of clay particles in the Upnor Formation, London Basin. Orsett Quarry, OQ1 (E434S1/02).





Plate 9: Root channel filled by well sorted clean sand grains in the Upnor Formation, London Basin. Orsett Quarry, OQ1 (E434S1/04).

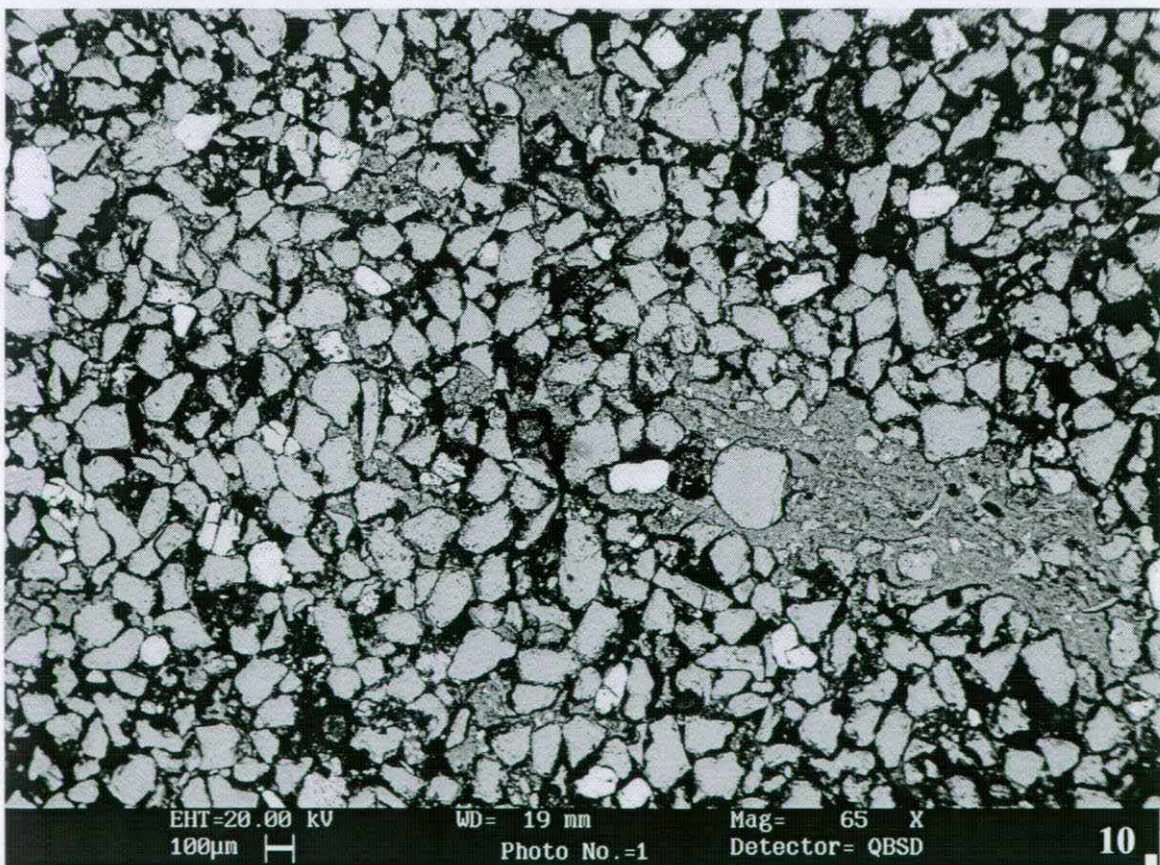


Plate 10: Poorly cemented, fine grained, glauconitic sand from the base of the Upnor Formation in Jubilee Line Extension BH 404T (40.35 m). Glauconite grains are light grey, quartz grains are mid grey with the enclosing clay matrix and clay laminae dark grey. Note the open pore network. (D785P1/01)



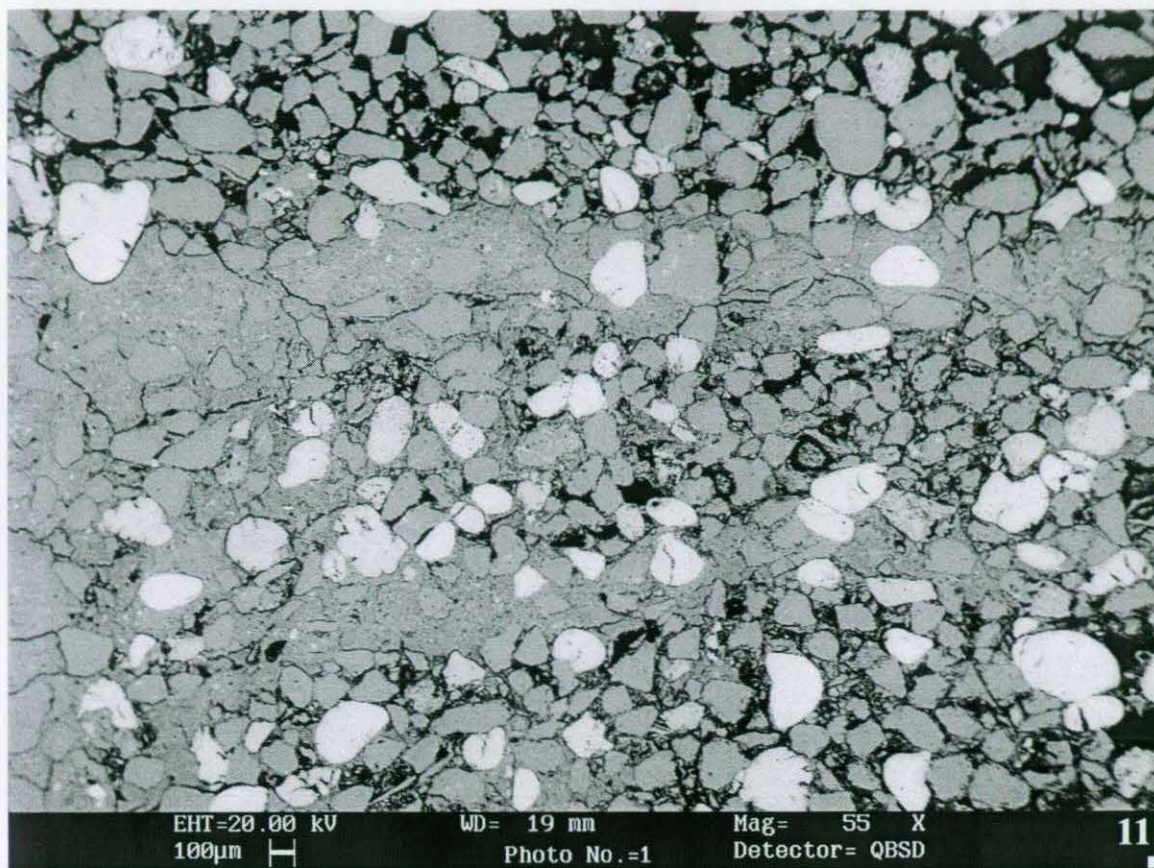


Plate 11: Glauconitic sand with clay laminae from the Upnor Formation in Jubilee Borehole 404T (38.01 m depth). Note the open porosity in the sandy areas and reduced porosity in the clay lenses. (D784P1/06)

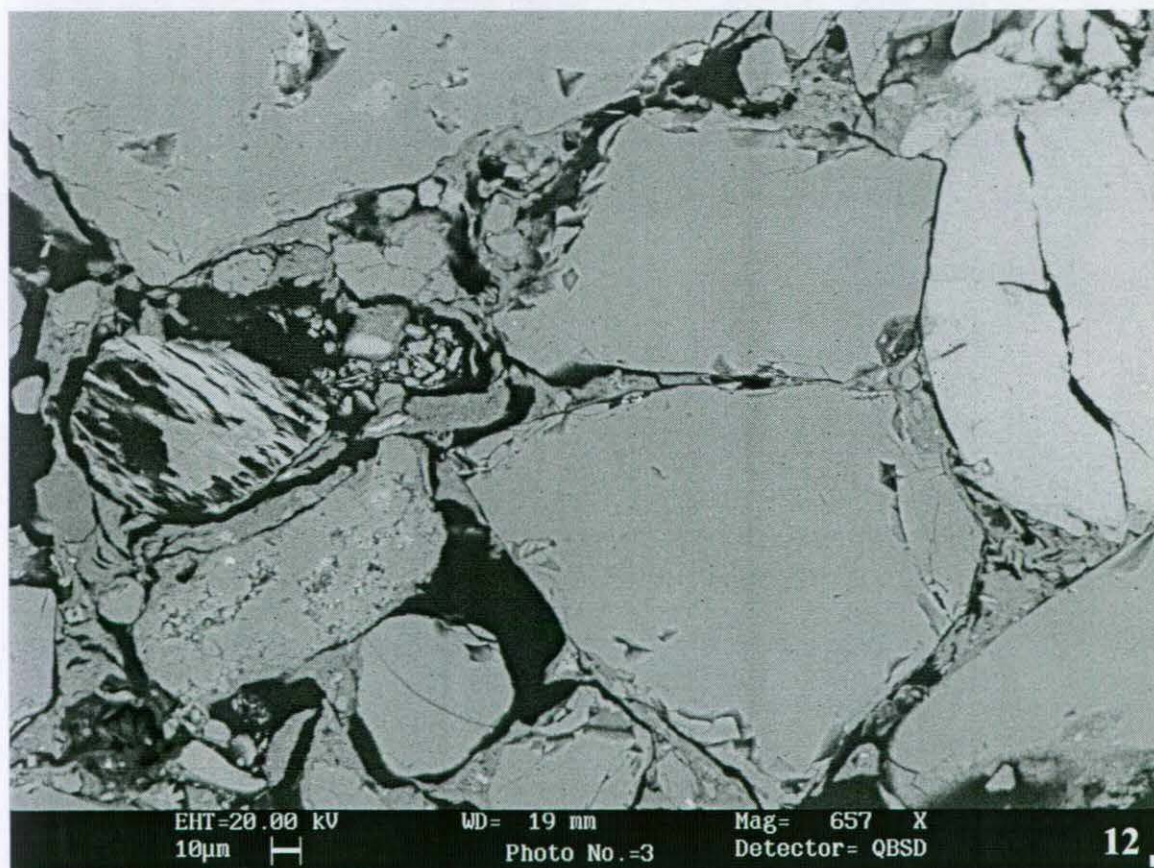


Plate 12: Typical detailed view of glauconitic sand from the Upnor Formation in Jubilee Borehole 404T (38.01 m depth). Note corroded albite grain, angular quartz grains and glauconite grain (right) with pores lined by smectitic clay. (D784P1/03)



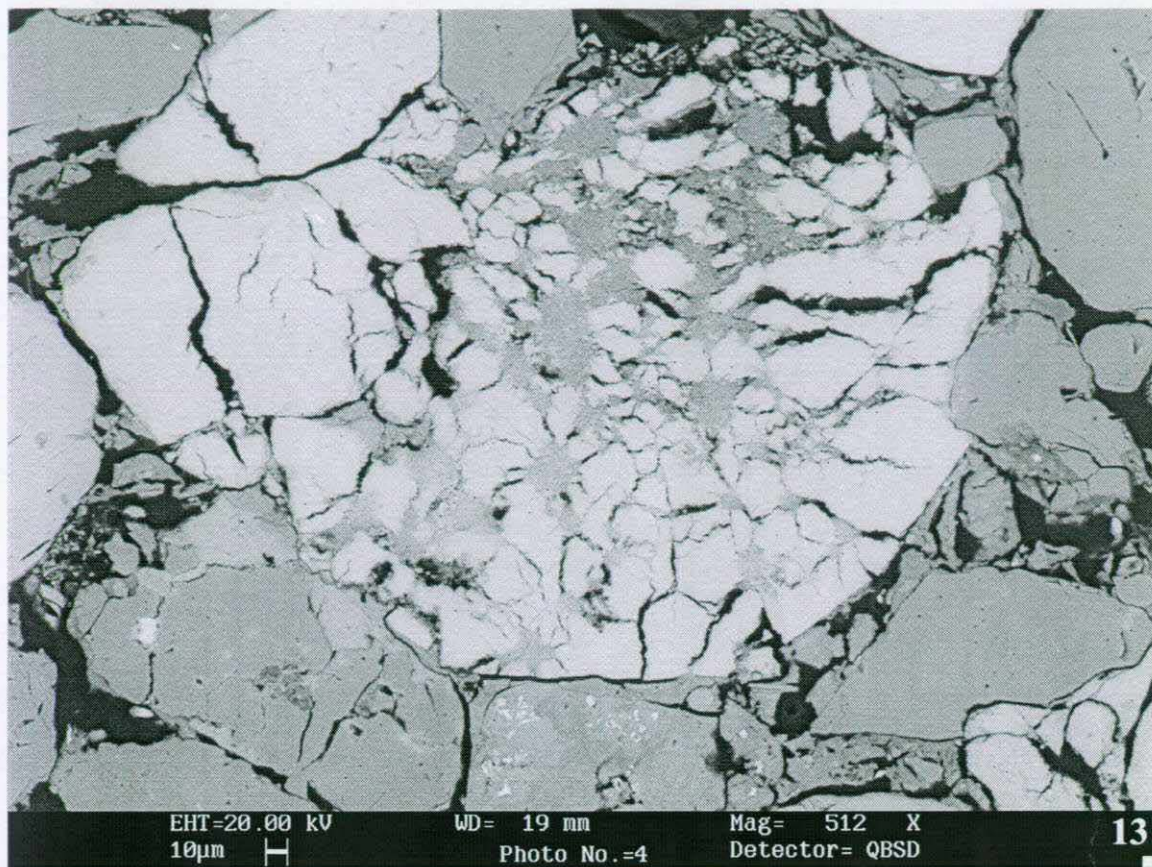


Plate 13: Glauconite pellet containing a calcium phosphate (collophane or apatite?) from the Upnor Formation in Jubilee Line Extension BH 404T (38.01 m depth). The extensive cracking may be due to drying induced shrinkage. (D784P1/04)

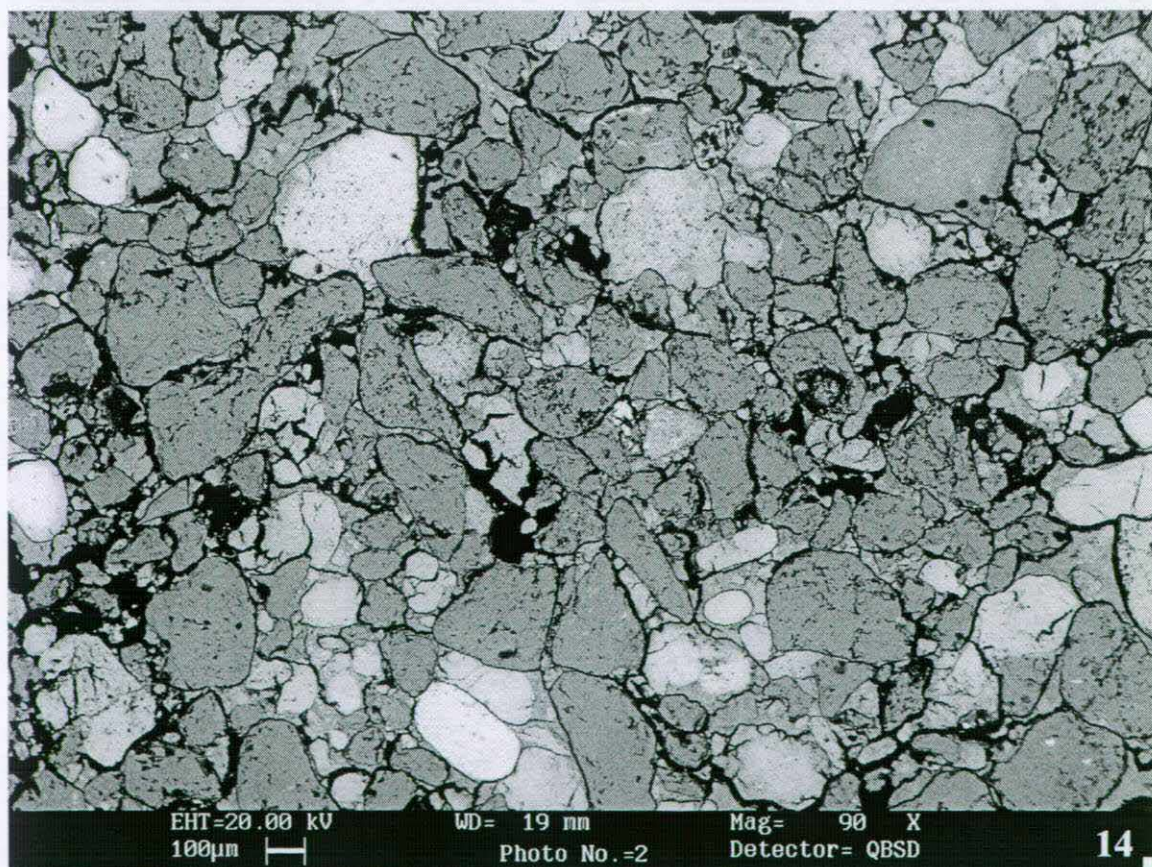


Plate 14: Example of the clay-rich glauconitic sands from the Upnor Formation. Note oxidised glauconite grains (light grey) and secondary porosity (much of which is thought to be drying artifacts prior to specimen preparation). Jubilee Line Extension BH 404T (36.30 m depth). (D783P1/02)



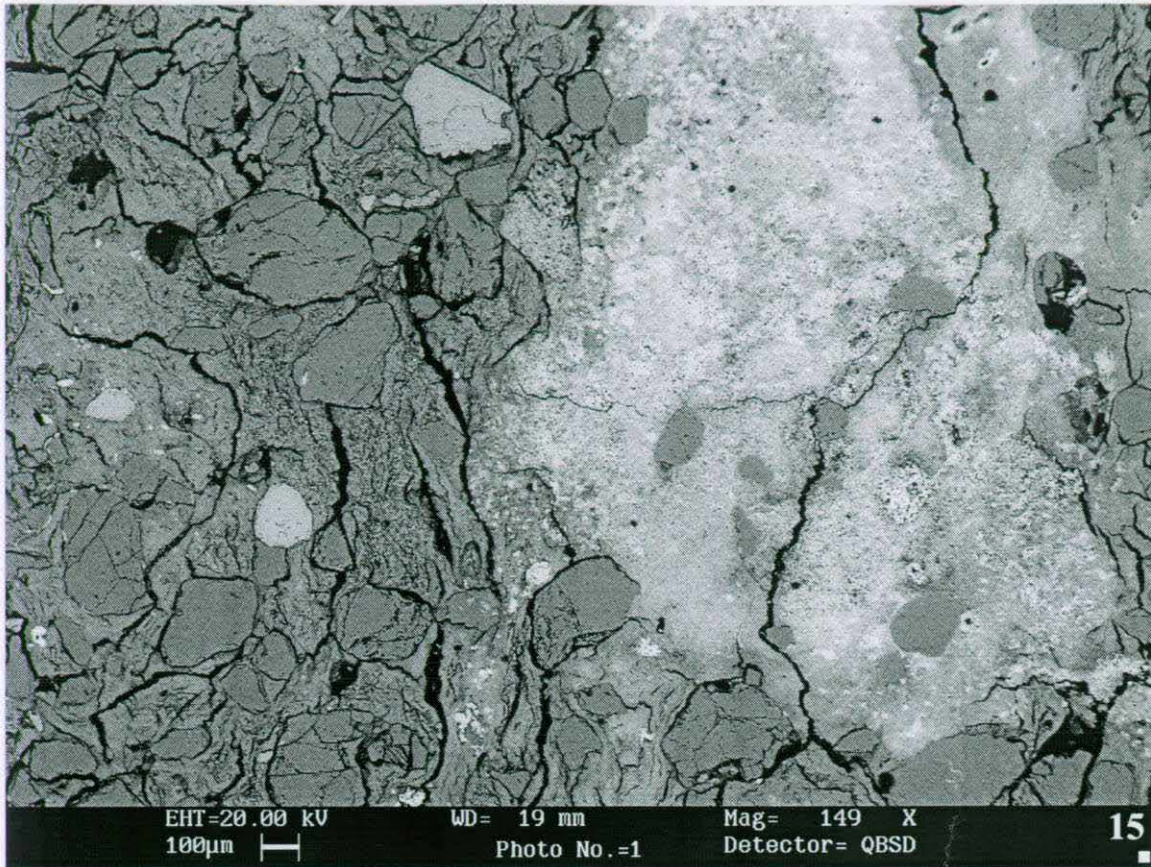


Plate 15: Example of the sandy clay from the upper part of the Upnor Formation with iron oxide staining (light grey areas on right half of image) accounting for the yellow staining seen in hand specimen. Up is from right to left. Jubilee Line Extension BH 404T (35.40 m depth). (D780P1/01)

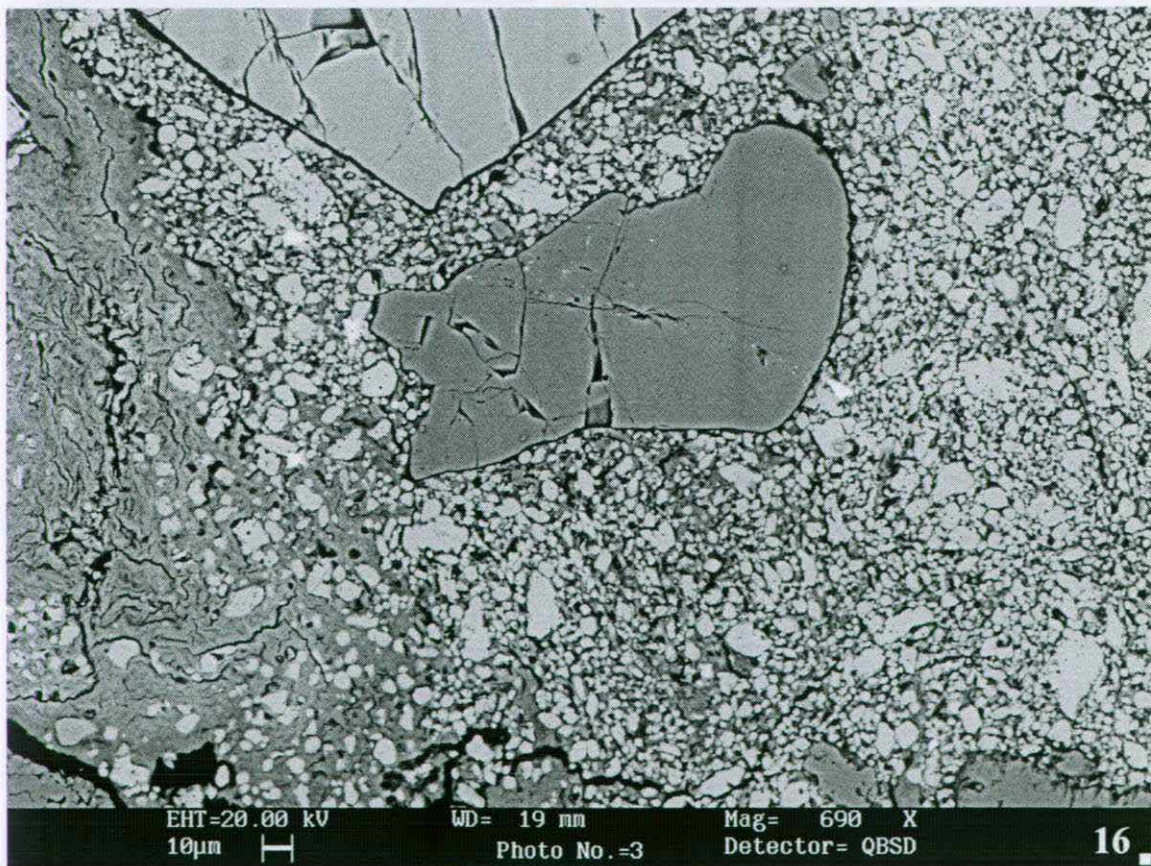


Plate 16: Detail of calcite concretions in the sandy clay from the upper part of the Upnor Formation. Up is from right to left. Jubilee Line Extension BH 404T (35.60 m depth). (D781P1/03)



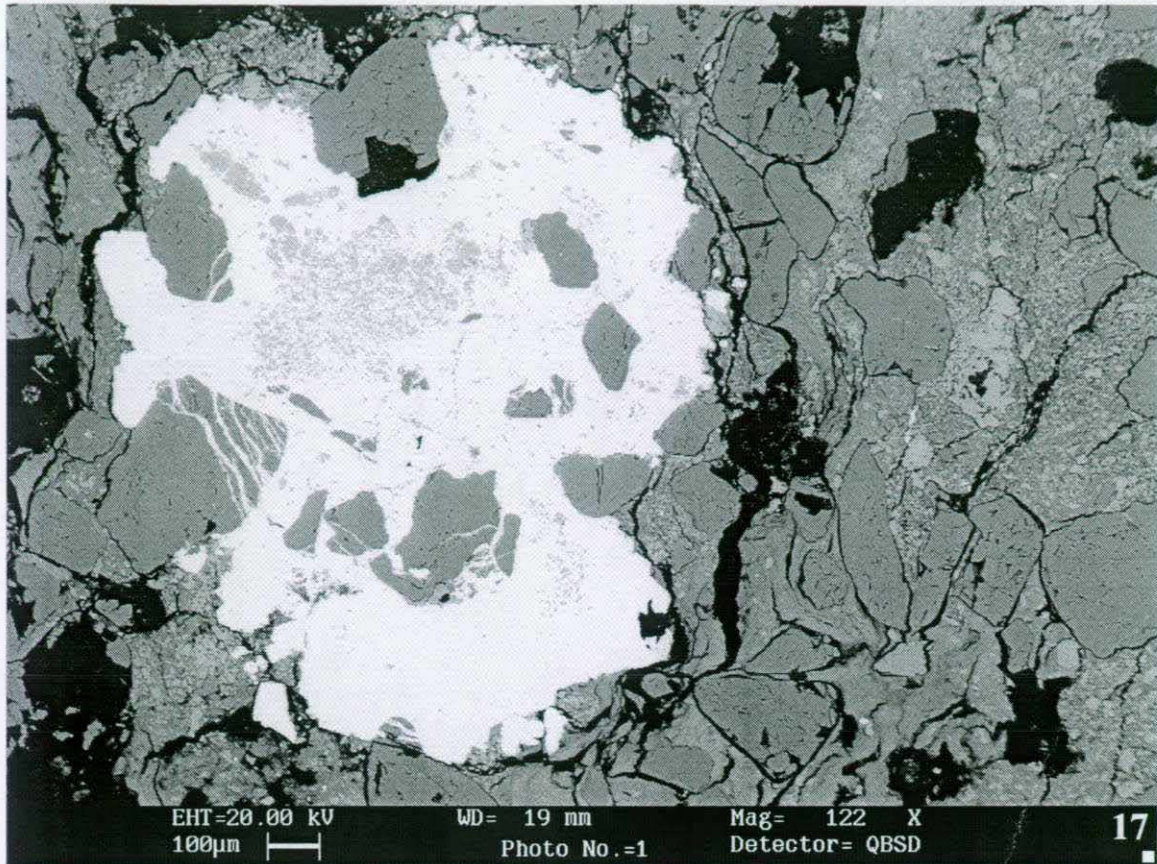


Plate 17: Pyrite and calcite concretion in the upper part of the Upnor Formation possibly replacing the original clay matrix. Note that quartz grains have been fractured and then sealed by the pyrite. Jubilee Line Extension BH 404T (35.60 m depth). (D781P1/01)

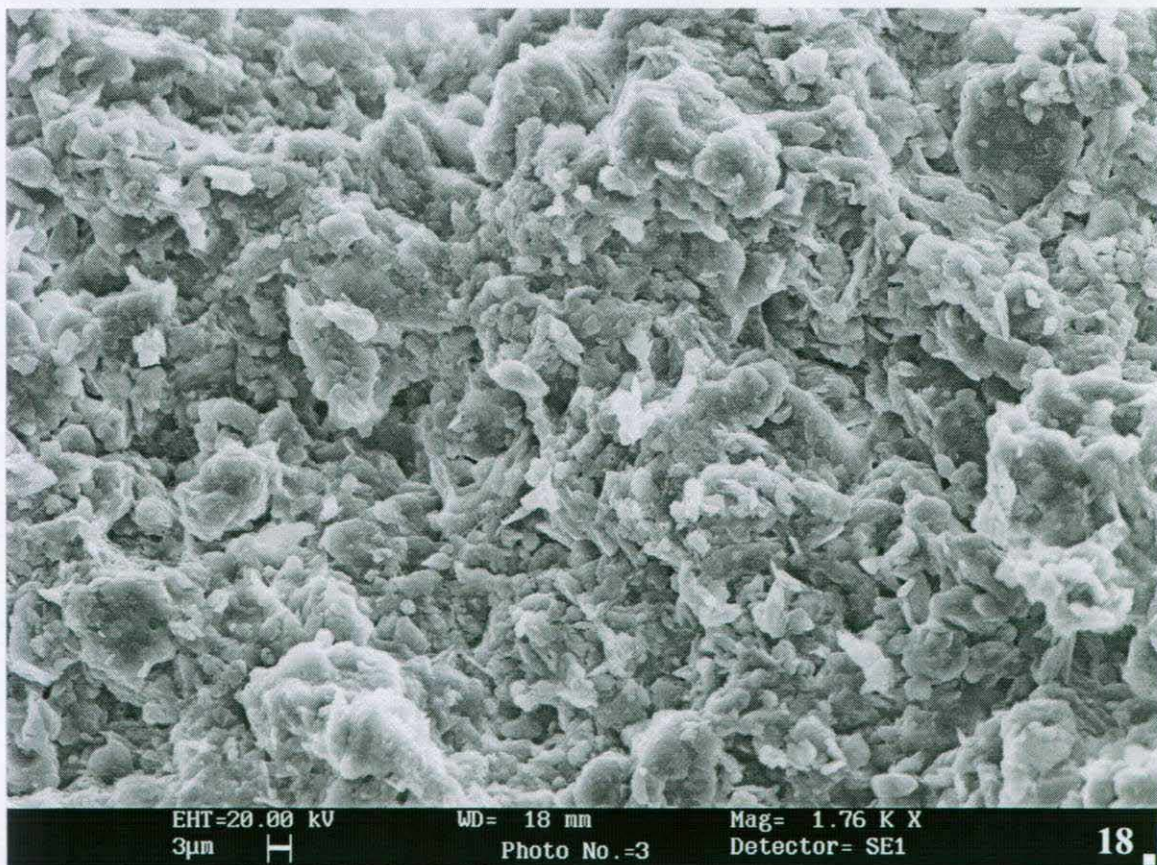


Plate 18: Typical example of a sandy clay from the Reading Formation in the London Basin comprising detrital fine sand-sized grains in a clay matrix consisting of (in this example) major illite and kaolinite with minor smectite. Sample NB16, Newbury Bypass Site E, 19.7 m above Chalk. (E442S1/03)



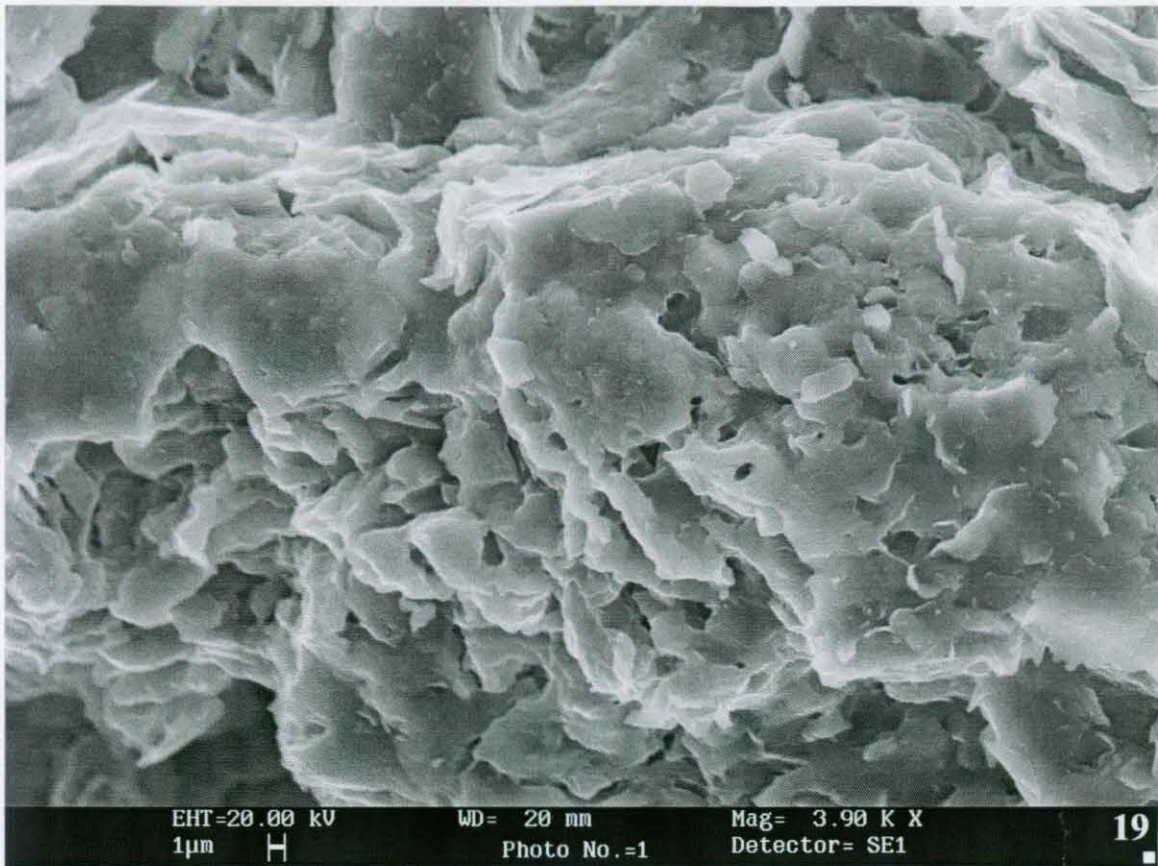


Plate 19: Corroded K-feldspar in the Reading Formation of the London Basin. Sample NB16, Newbury Bypass Site E, 19.7 m above Chalk. (E442S1/01)

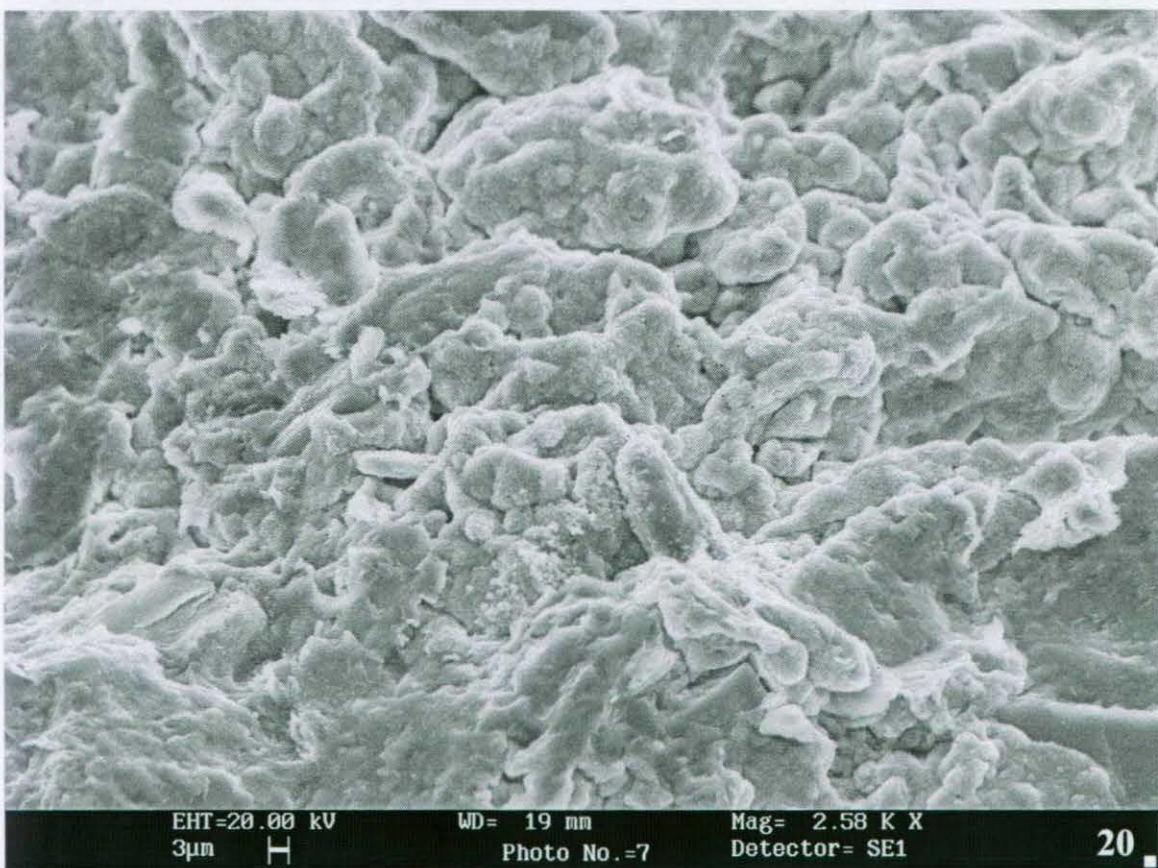


Plate 20: Clay matrix in the Reading Formation of the London Basin, in which the clay minerals (here major smectite with minor kaolinite and illite) occur in silt-sized aggregates. Note the relatively open porosity compared to plates 15 and 16. Sample NB1, Newbury Bypass Site A, 2.25 above Chalk m. (E438S1/07)



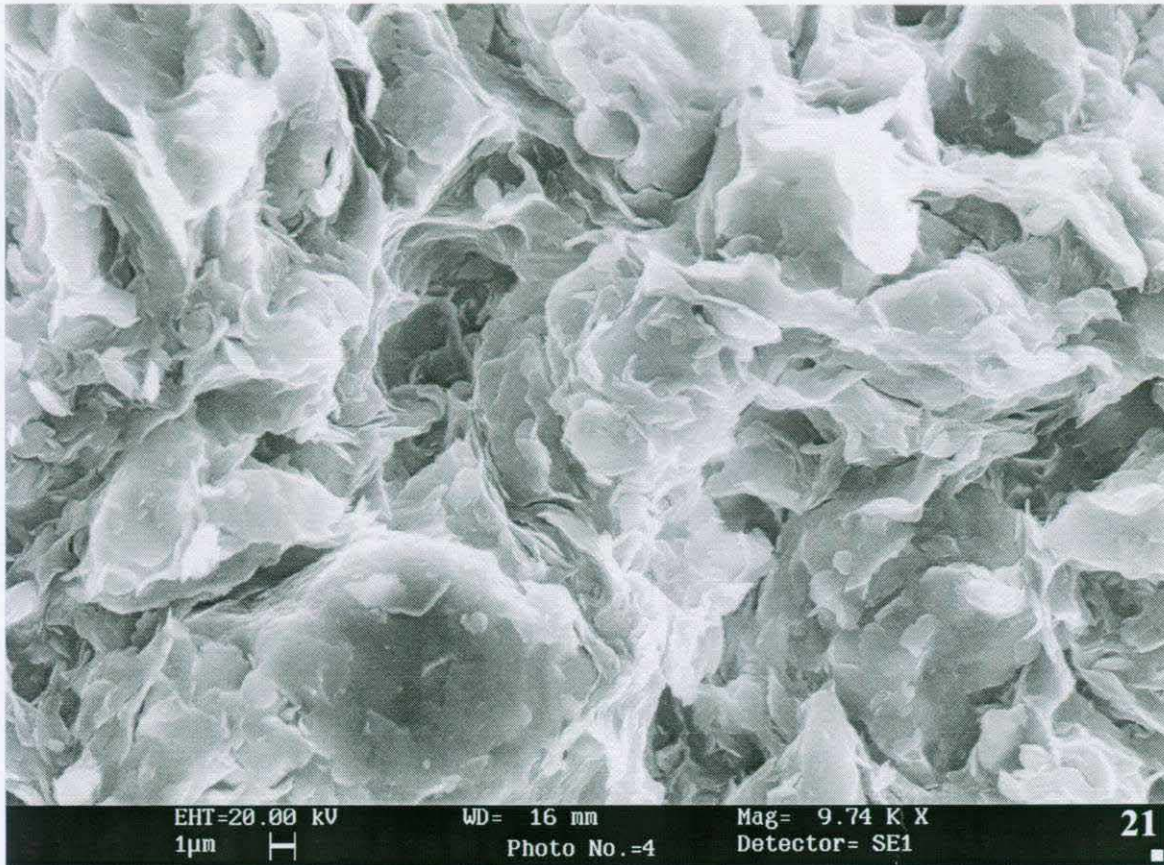


Plate 21: Detailed view of randomly oriented ragged clay flakes (here major smectite, minor illite and kaolinite) in the Reading Formation of the London Basin. Sample NB27C, Newbury Bypass 13.6 m above Chalk. (E443S1/04)

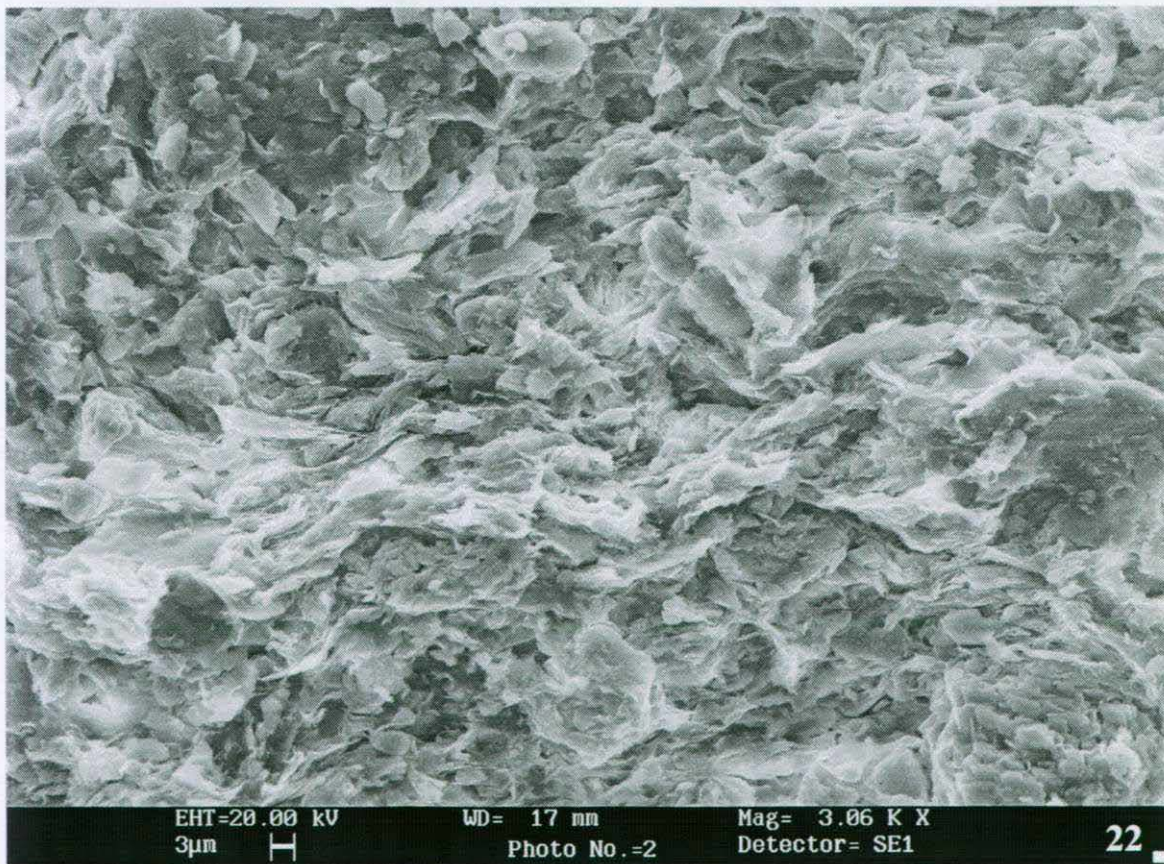


Plate 22: Example of a very weakly developed laminated sedimentary fabric in the Reading Formation of the London Basin. Sample NB7, Newbury Bypass 5.35 m above Chalk. (E440S1/02)



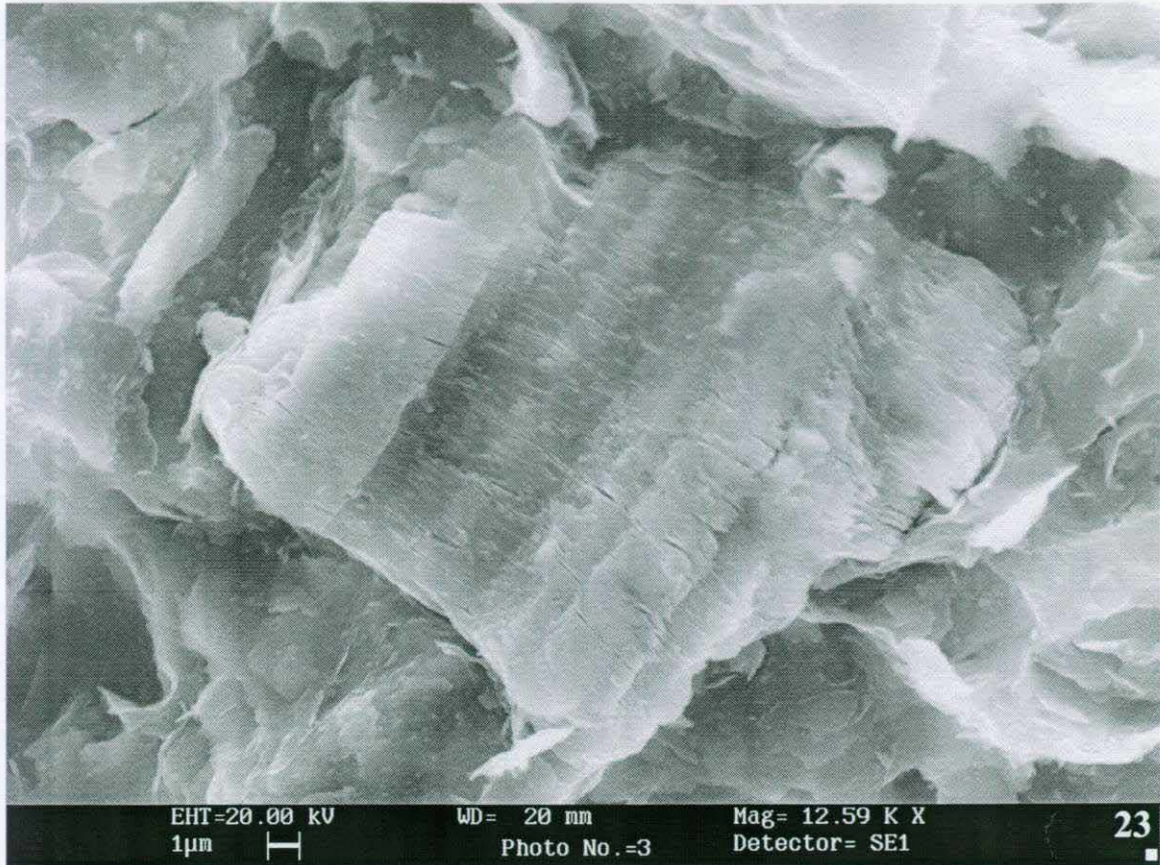


Plate 23: A rare well developed kaolinite book within the clay matrix of the Reading Formation of the London Basin. Sample M40. (E444S1/03)

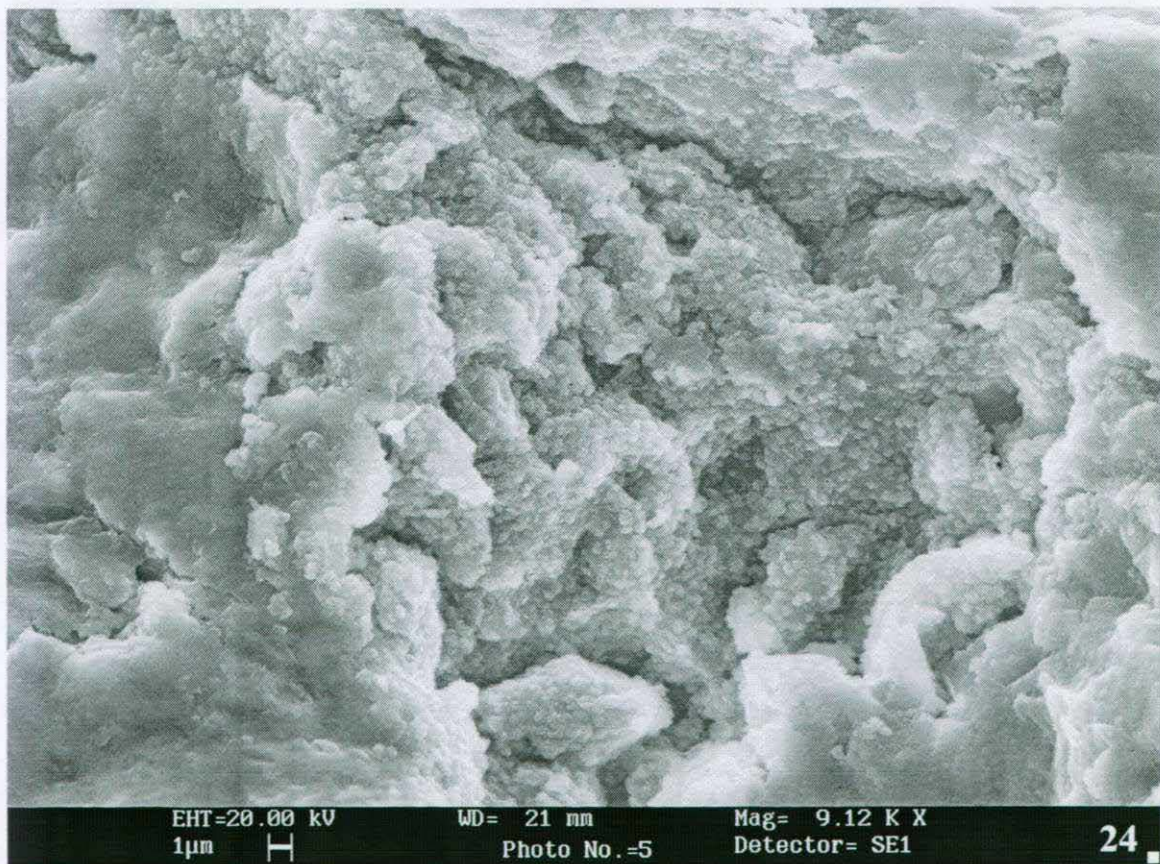


Plate 24: Fine-grained microbotryoidal iron oxyhydroxide lining large void in Reading Formation of the London Basin. Sample NB1, Newbury Bypass 2.25 m above Chalk. (E438S1/05)



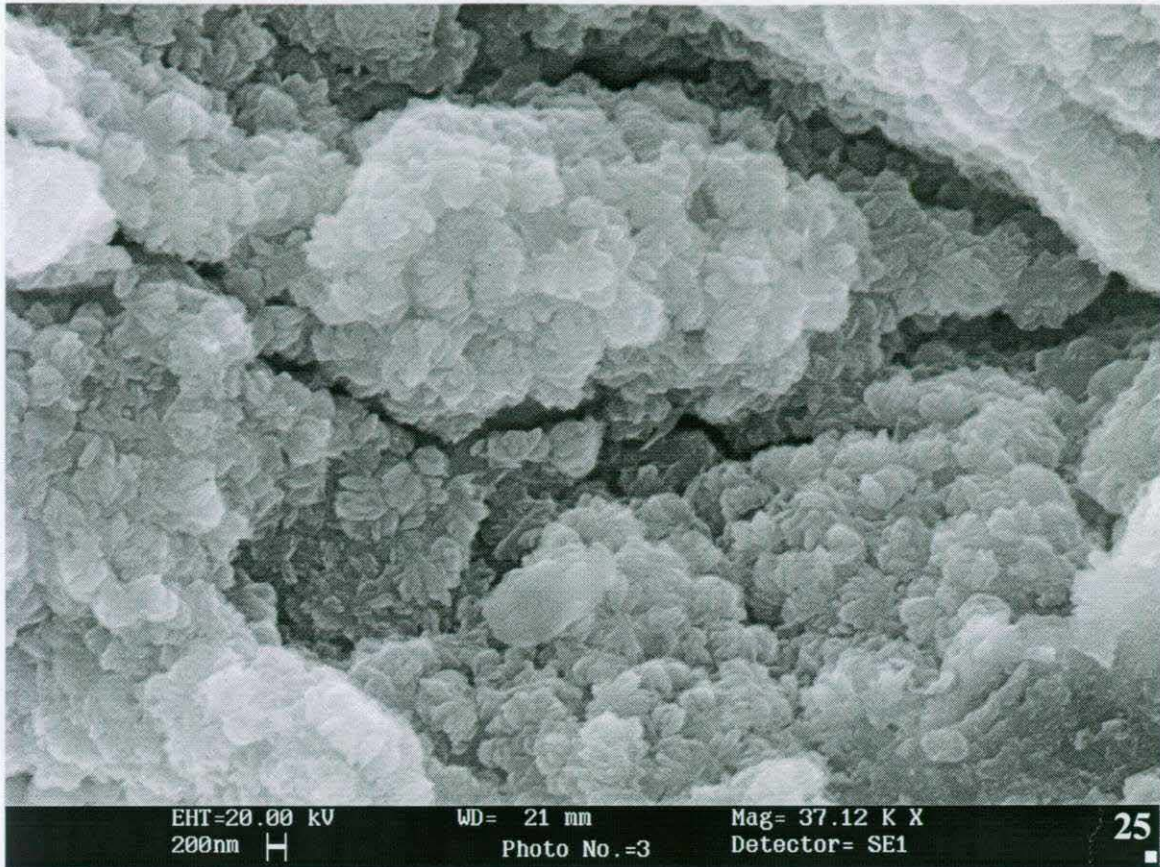


Plate 25: Detailed view of iron oxyhydroxide habit lining large void in Reading Formation of the London Basin. Sample NB1, Newbury Bypass 2.25 m above Chalk. (E438S1/03)

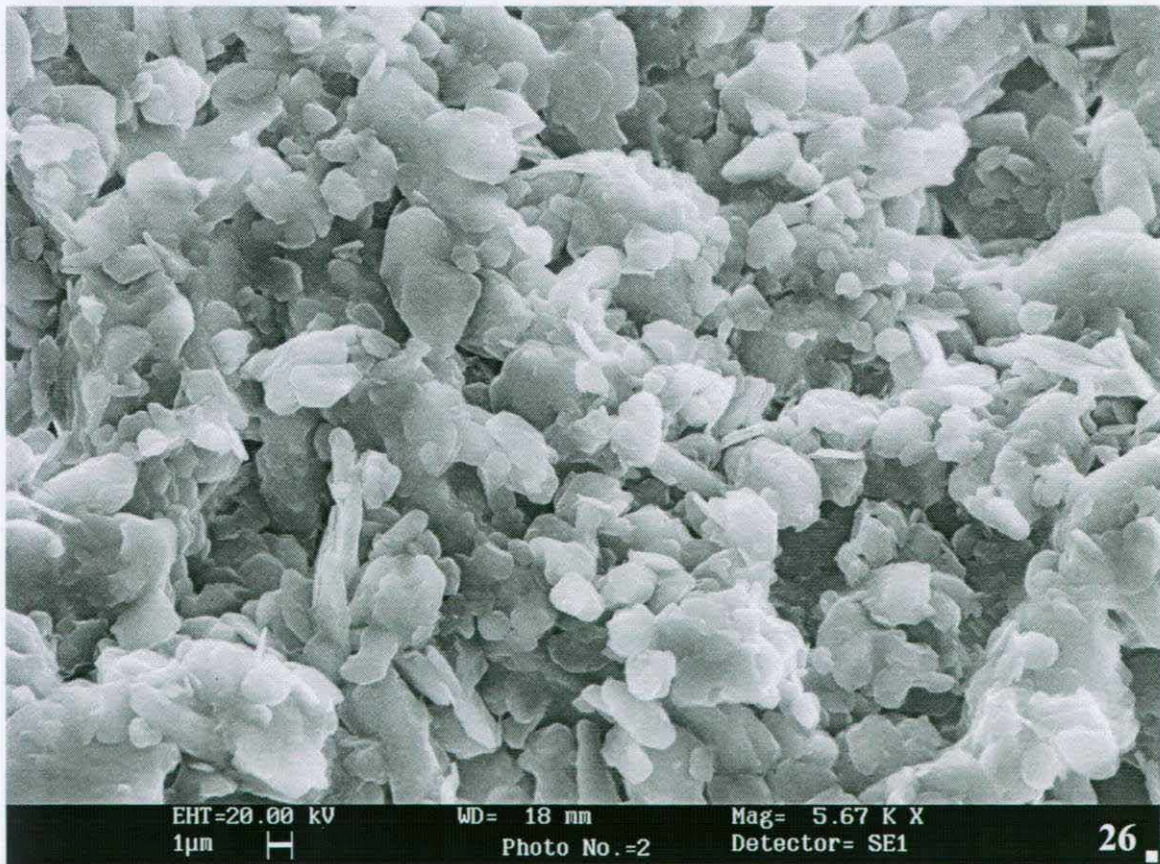


Plate 26: Irregular, micron-scale silica crystals forming a void-lining in the Reading Formation of the London Basin. Sample NB16, Newbury Bypass Site E, 19.70 m above Chalk. (E442S1/02)



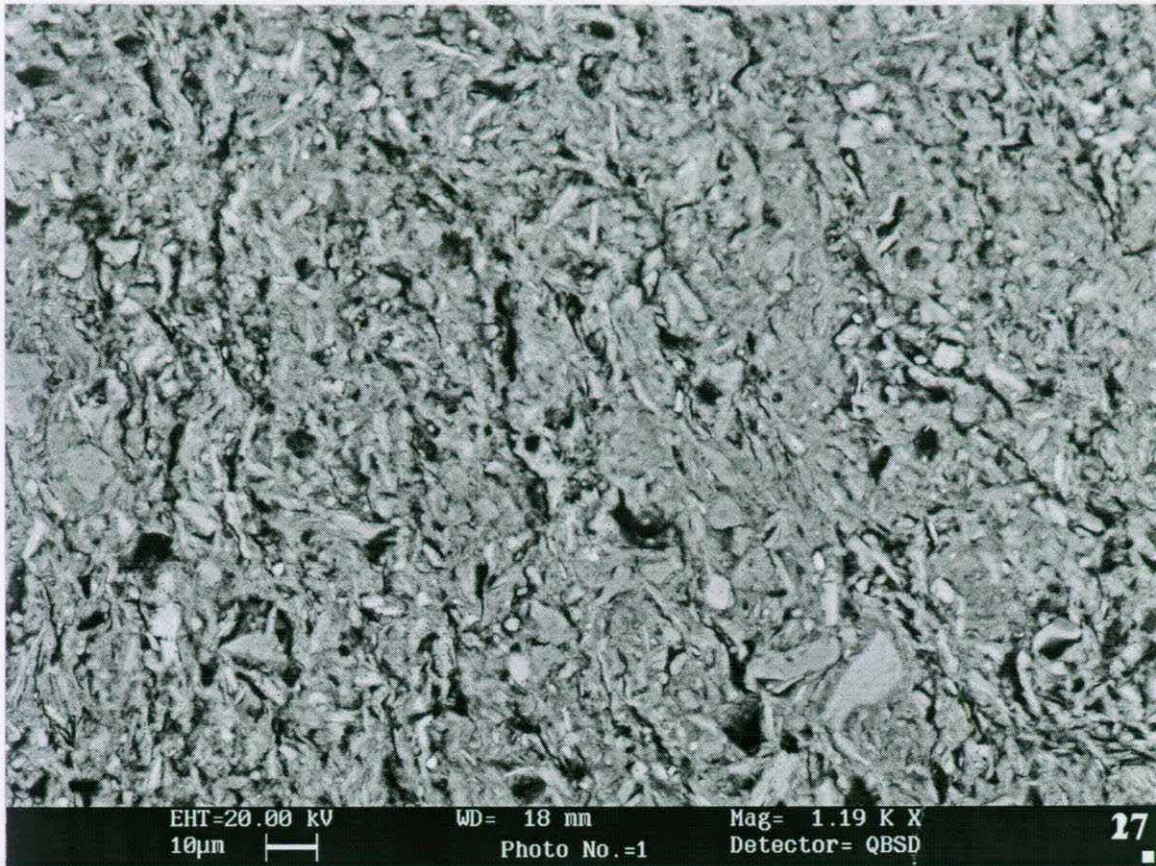


Plate 27: Typical view of blue-grey clay from the Upper Mottled Clay of the Reading Formation in the London Basin. Sample JLE26.3 m, Jubilee Line Extension borehole 404T. (D501/01)

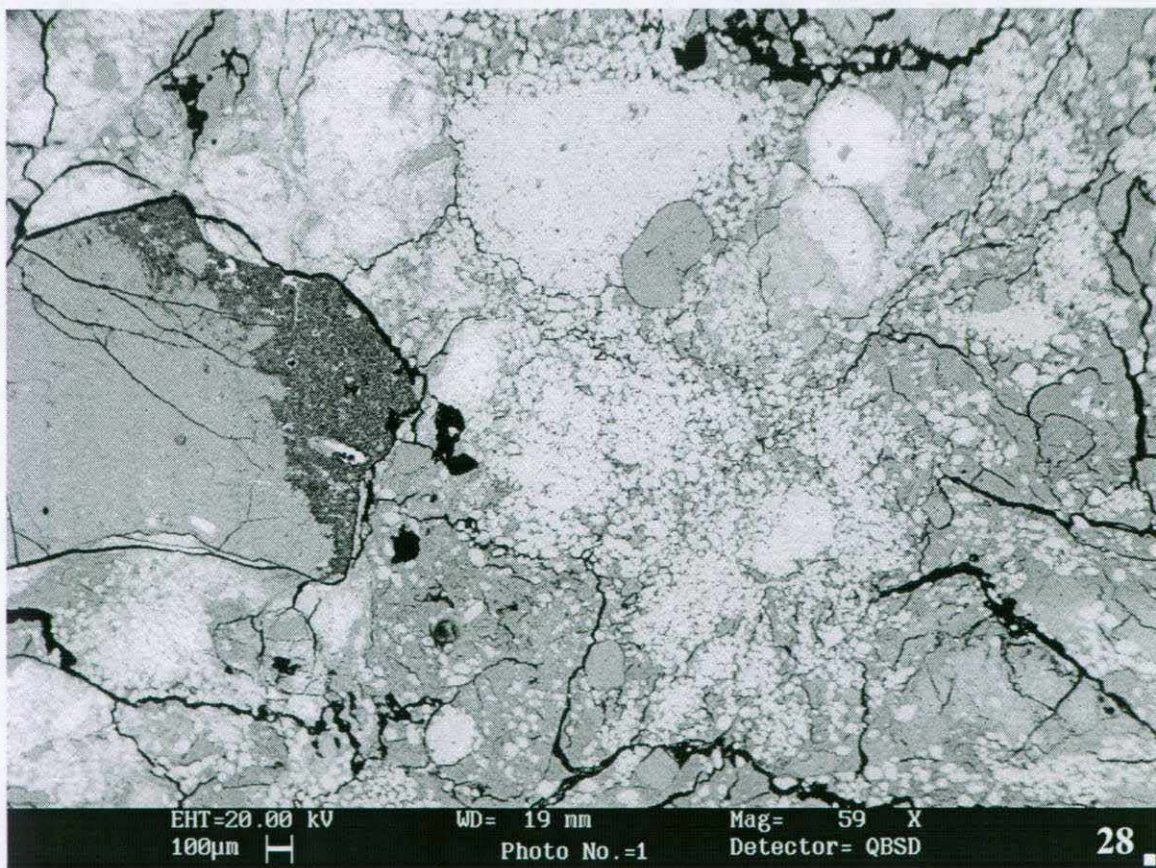


Plate 28: Lower Mottled Clay in the Reading Formation. The original clay has been patchily altered to leave a siliceous matrix (dark grey) and pervasively stained by iron oxide (light grey). Calcite rhombs (mid grey) form concretions. Sample JLE 34.20, Jubilee Line Extension BH 404T. (D777P1/01)



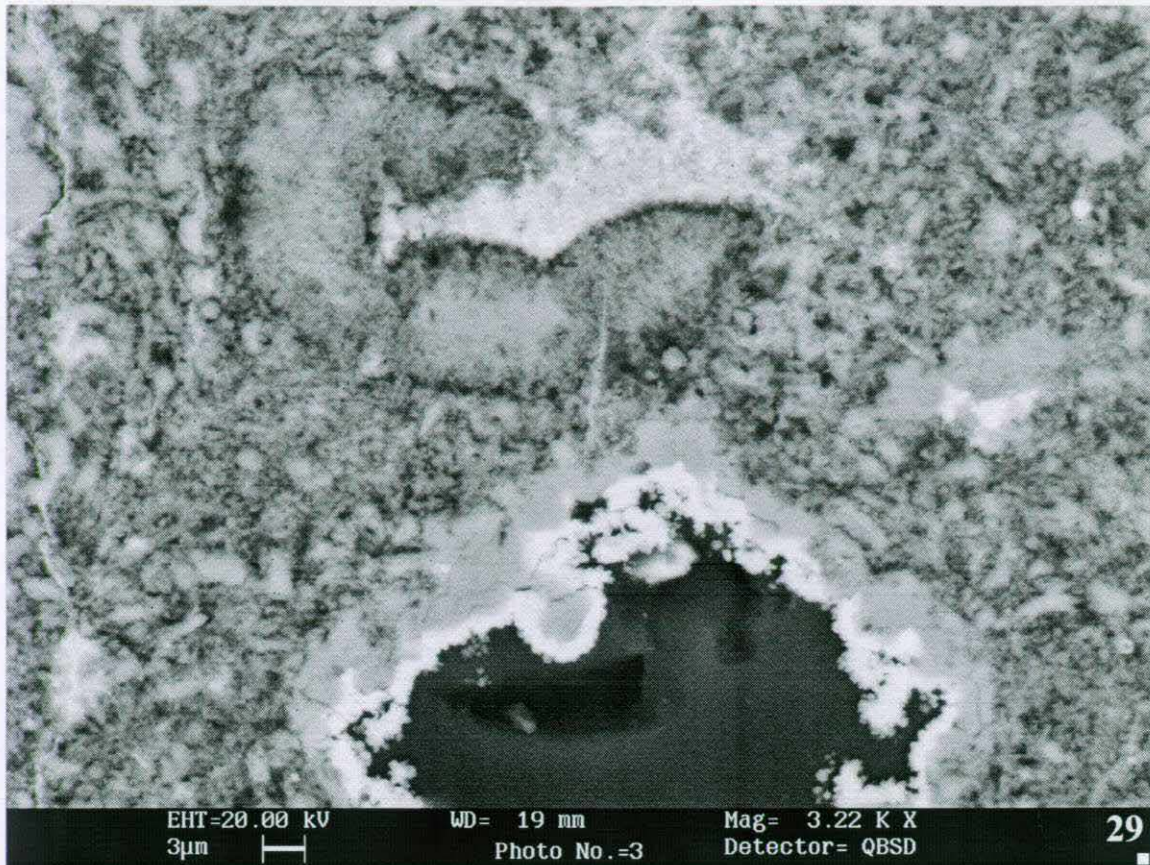


Plate 29: Detail of clay which has been altered to a siliceous matrix. Note the void is lined by colloform silica and subsequently by iron oxide. Sample JLE 34.20 , Jubilee Line Extension BH 404T. (D777P1/03)

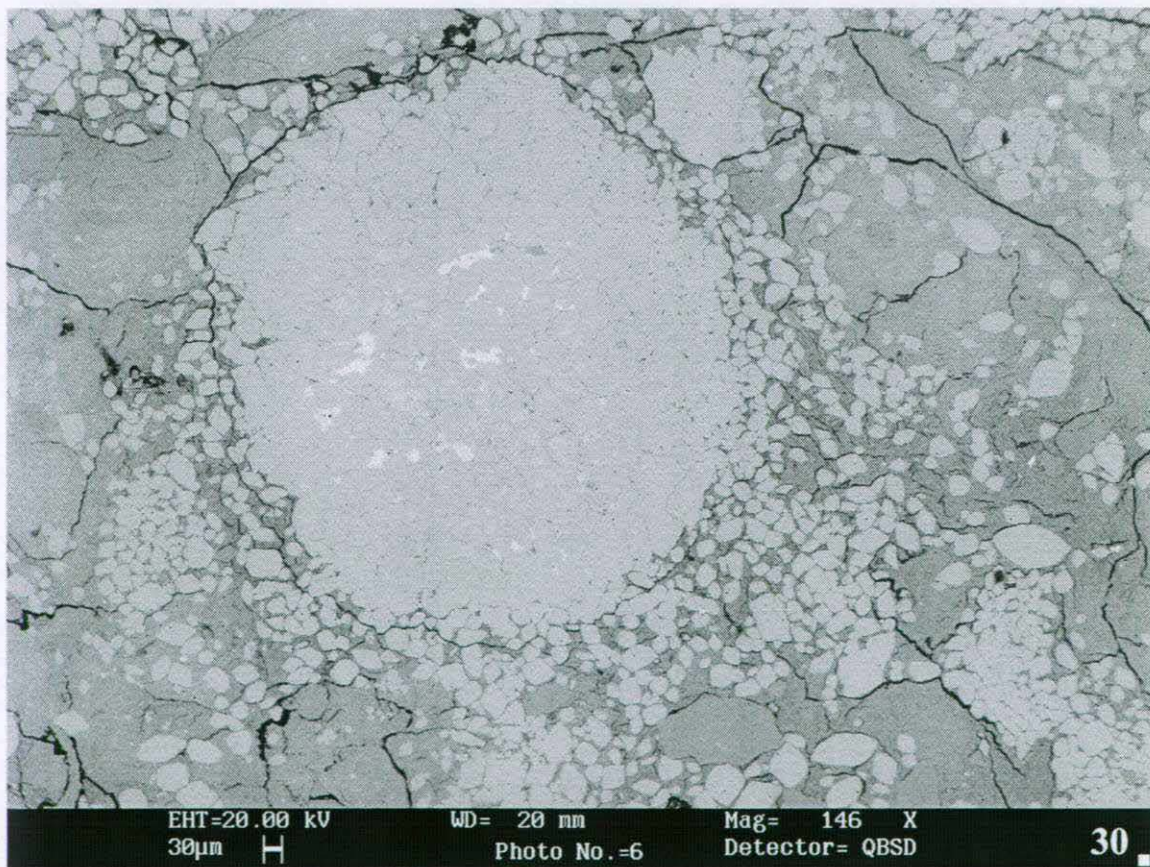


Plate 30: A calcite concretion and extensive precipitation of calcite rhombs within the clay. Note enclosed iron oxide. Sample JLE 34.20 , Jubilee Line Extension BH 404T. (D777P1/06)



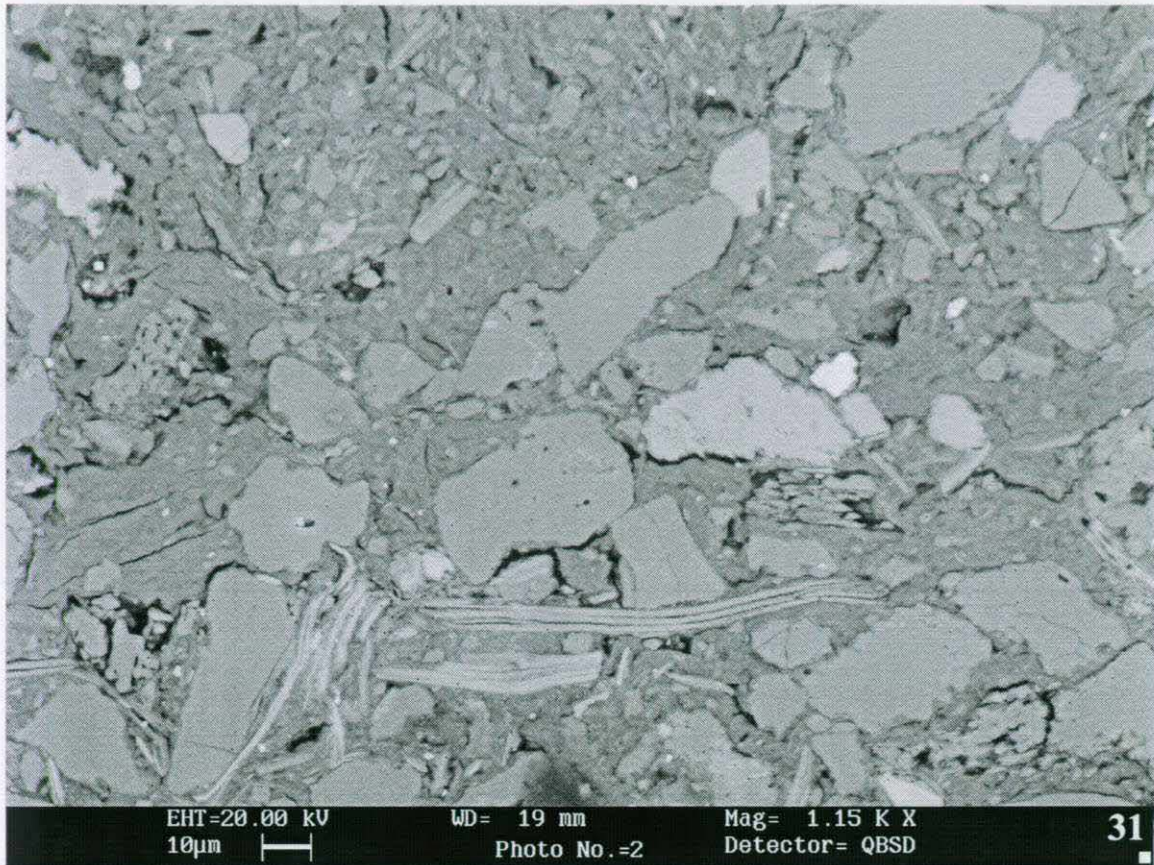


Plate 31: Sand-rich clay laminae in the Laminated Sands and Silts of the Woolwich Formation. Note corroded feldspars and expanded mica. Sample JLE 30.05 m , Jubilee Line Extension BH 404T. (D772P1/02)

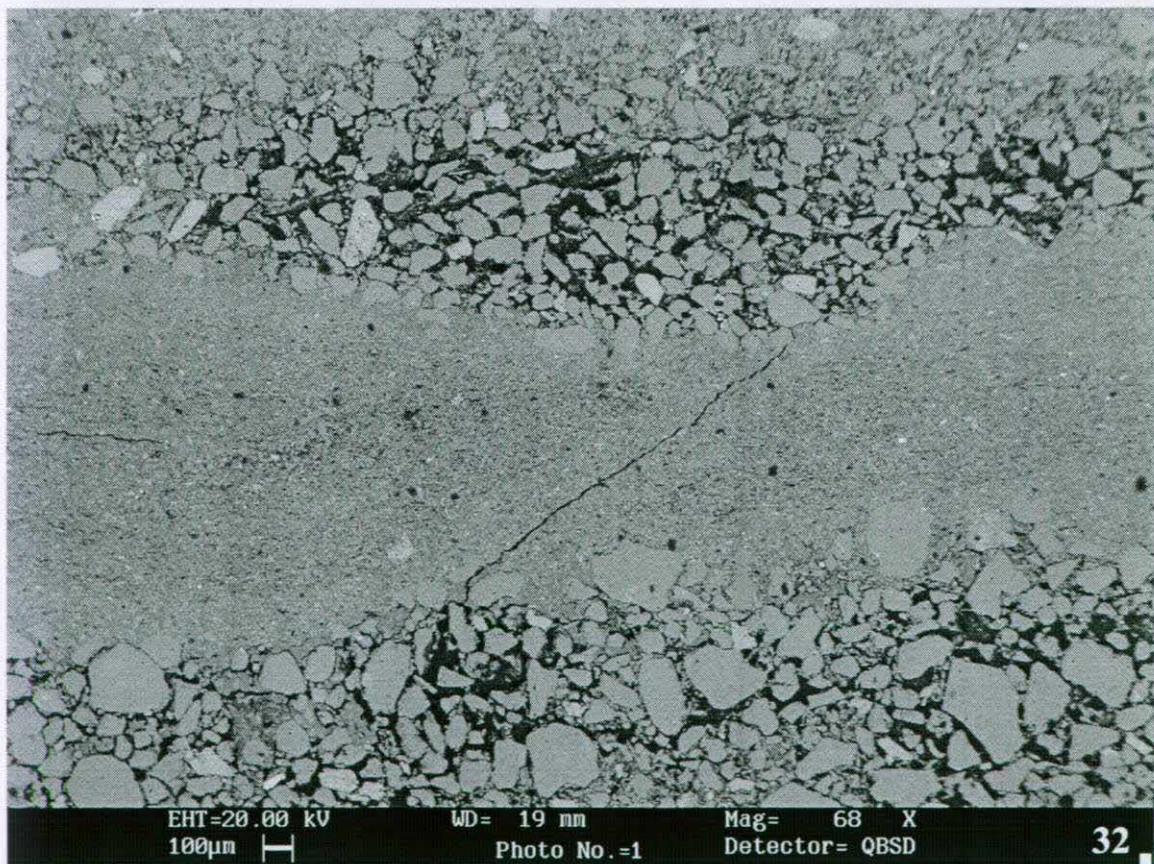


Plate 32: Clay, sandy-clay and sand laminae in the Laminated Sands and Silts of the Woolwich Formation. Note variable porosity. Sample JLE 30.05 m , Jubilee Line Extension BH 404T. (D772P1/01)



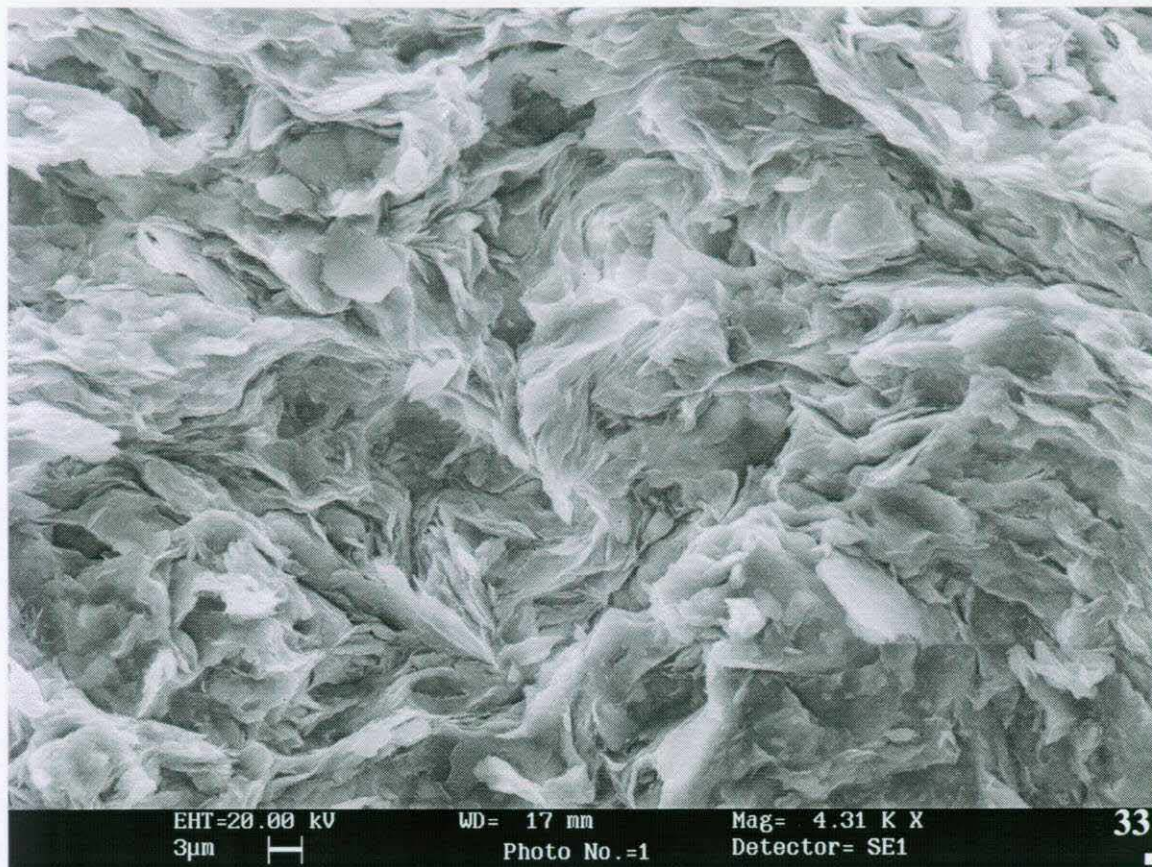


Plate 33: Typical view of clay matrix, comprising major illite with minor kaolinite and smectite in the Upnor Formation from Alum Bay, Isle of Wight (6.0 m above Chalk). (D816S1/01)

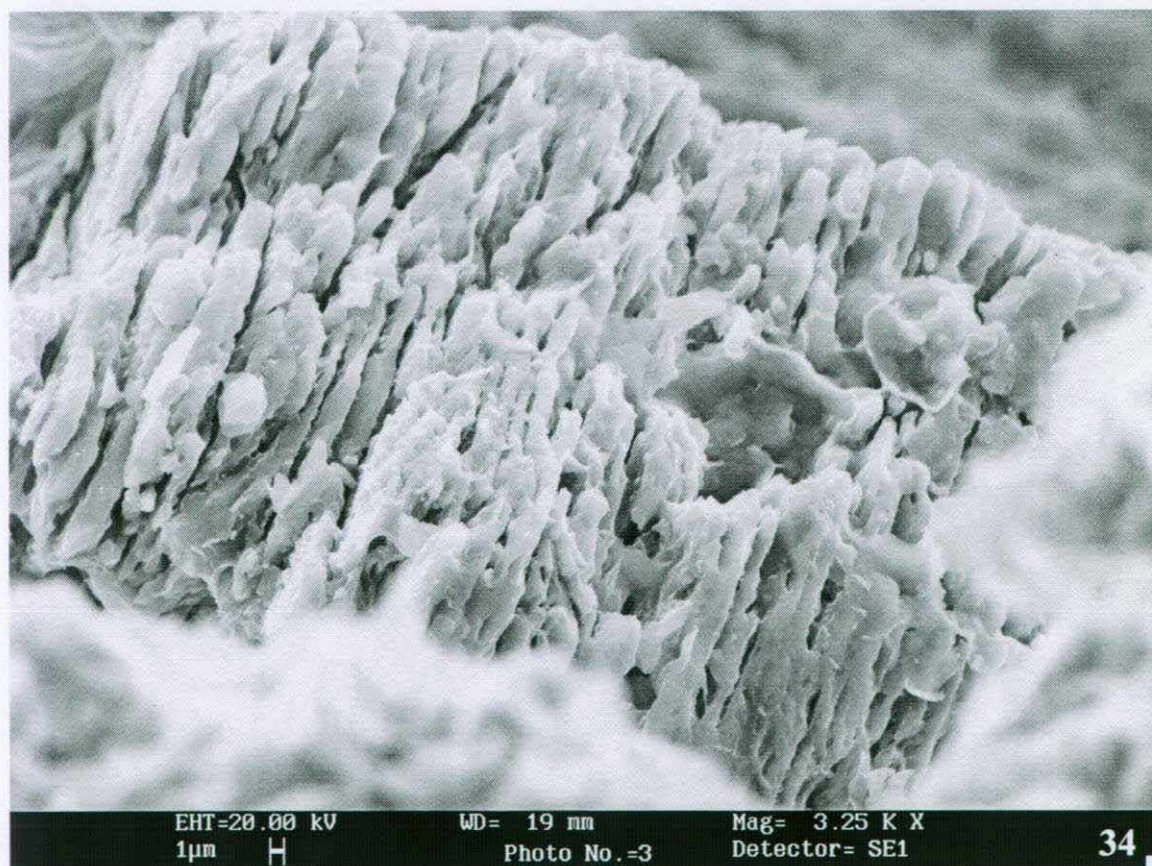


Plate 34: Rare, coarse corroded kaolinite book in the Reading Formation of the Hampshire Basin in Alum Bay, Isle of Wight (17.6 m above Chalk). (D821S1/03)



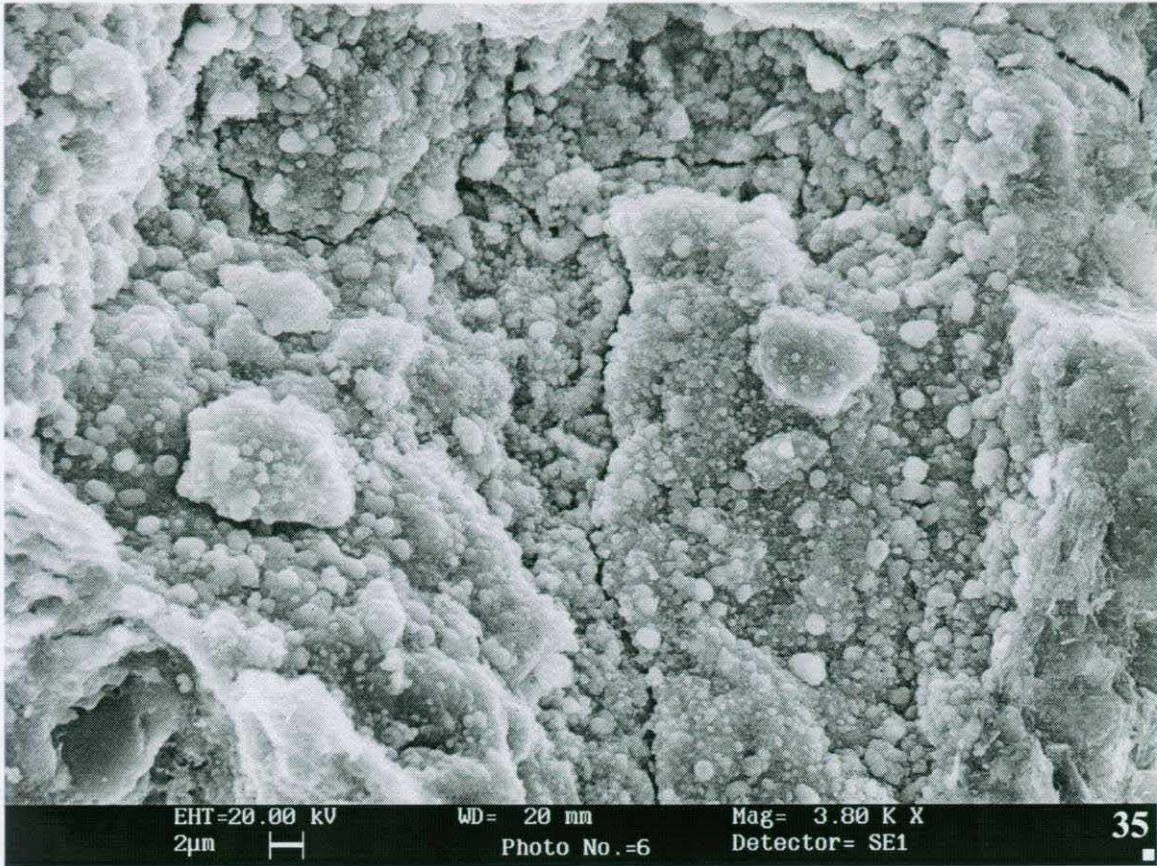


Plate 35: Anhedronal to occasionally micro-botryoidal goethite lining voids in the Reading Formation of the Hampshire Basin in Alum Bay, Isle of Wight (17.6 m above Chalk). (D821S1/06)



Plate 36: Hematite rosettes forming thin linings on voids in the Reading Formation of the Hampshire Basin in Alum Bay, Isle of Wight (18.9 m above Chalk). (D822S1/04)





# BRITISH GEOLOGICAL SURVEY

## REPORT APPROVAL FORM

British Geological Survey  
Kingsley Dunham Centre  
Keyworth  
Nottingham  
United Kingdom  
NG12 5GG

Tel (0115) 9363100  
Fax (0115) 9363200

Report Title and Authors

The mineralogy and petrography of the Lambeth Group from the London and Hampshire Basins

Pearce, JM, Kemp, SJ and Hards, VL

Client Name and Address

Client Report No.

BGS Report No. WG/98/4R

Client Contract Ref.

BGS Project Code E72FZA12

Classification Open

Version	Status	Prepared by	Checked by	Approved by	Date
1		<i>JM Pearce</i>	<i>V.L. Hards</i>	<i>S.J. Kemp</i>	5/7/99